

Revisiting fermion mass and mixing fits in the minimal SUSY $SO(10)$ GUT

Takeshi Fukuyama,¹ Koji Ichikawa,² and Yukihiro Mimura³

¹*Research Center for Nuclear Physics (RCNP), Osaka University,
Ibaraki, Osaka, 567-0047, Japan*

²*University of Tokyo,*

*Kavli Institute for the Physics and Mathematics of the Universe (KIPMU)
5-1-5 Kashiwa-no-Ha, Kashiwa Shi, Chiba 277-8568, Japan*

³*Department of Physics, National Taiwan University, Taipei, 10617, Taiwan*

Abstract

The supersymmetric $SO(10)$ grand unified models with renormalizable Yukawa couplings involving only $\mathbf{10}$ and $\overline{\mathbf{126}}$ Higgs fields have been shown to realize the fermion masses and mixings economically. In previous works, the sum rule of the fermion mass matrices are given by inputting the quark matrices, and the neutrino mixings are predicted in the framework. Now the three neutrino mixings have been measured, and in this paper, we give the sum rule by inputting the lepton mass matrices, which makes clear to show the feature of the solution, especially if the vacuum expectation values of $\mathbf{126} + \overline{\mathbf{126}}$ (v_R) are large and the right-handed neutrinos are heavy. We perform the χ^2 analyses to fit the fermion masses and mixings using the sum rule. In the previous works, the best fit appears at $v_R \sim 10^{13}$ GeV, and the fit at the large v_R scale ($\sim 10^{16}$ GeV) has been less investigated. We discuss the possible low energy threshold correction of the sum rule and the proton decay suppression, which makes the large v_R solution still attractive. Using the fit results, we perform the calculation of the $\mu \rightarrow e\gamma$ process and the electric dipole moment of electron, and the importance of v_R dependence emerges in the low energy phenomena. We also show the prediction of the CP phase in the neutrino oscillations, which can be tested near future.

PACS. 12.10.-g, 12.10.Dm, 12.10.Kt

1 Introduction

The Higgs discovery at LHC [1] opens a new era to understand the fermion masses and the mixings, which are generated by the Yukawa interaction to the Higgs boson. Indeed, most of the parameters in the standard model (SM) lie in the Yukawa coupling matrices. The difference of the generation mixings between quark and lepton sectors is one of the major issues to understand the structure in the Yukawa coupling matrices. The measurement of the 13 neutrino mixing angle by using the oscillations from the reactor neutrino [2] and the ongoing measurement of the CP phase in the neutrino oscillations [3] can fill the piece of the flavor puzzle and impose a test to the bunch of flavor models.

The supersymmetric grand unified theory (SUSY GUT) can provide the most promising framework to incorporate these vast data systematically and consistently. Among many candidates, $SO(10)$ [4] is the smallest simple gauge group under which the entire SM matter contents of each generation are unified into a single anomaly-free irreducible representation, $\mathbf{16}$. The $\mathbf{16}$ -dimensional spinor representation in $SO(10)$ includes the right-handed neutrino and no other exotic matter particles. A particular attention has been paid to the renormalizable minimal $SO(10)$ model, where two Higgs multiplets $\{\mathbf{10} \oplus \overline{\mathbf{126}}\}$ are utilized for the Yukawa couplings with the matter representation [5]. The couplings to the $\mathbf{10}$ and $\overline{\mathbf{126}}$ Higgs fields can reproduce realistic charged fermion mass matrices using their phases thoroughly [6]. Surely, these mass relations are realized at GUT scale, and the evolution via renormalization group equations (RGEs) is considered to fit them with the low energy data of quark-lepton phenomena including the neutrino oscillations [7]. The Higgs superpotential has been also investigated to see the detail pattern of symmetry breaking from $SO(10)$ down to the SM gauge group [8, 9]. In these analyses, the criterion of the renormalizability plays an essential role not only to reduce the number of parameters but also to construct a model without the vacuum expectation values (vevs) of $B - L = \pm 1$ direction by $\mathbf{16}_H + \overline{\mathbf{16}}_H$ representations to break $SO(10)$ symmetry. Actually, the vevs of $B - L = \pm 2$ direction by $\mathbf{126} + \overline{\mathbf{126}}$ vevs reduces the rank of the gauge symmetry in the renormalizable model, in which the R -parity is automatically conserved in the minimal SUSY standard model (MSSM) vacua. The extension to include $\mathbf{120}$ Higgs representation without breaking the renormalizability has been also considered [10]. The $\overline{\mathbf{126}}$ Higgs representation includes both $SU(2)_L$ and $SU(2)_R$ triplets, and the Yukawa interaction to $\overline{\mathbf{126}}$ can generate both left- and right-handed Majorana neutrino mass matrices. Therefore, in the framework of the minimal $SO(10)$, depending on the symmetry breaking vacua, the light neutrino mass matrix can be obtained [11, 12] in both type I and II seesaw mechanism [13, 14].

Since the fermion mass matrices are given by the linear combination of two symmetric matrices (multiplied by doublet Higgs mixings), one can obtain the sum rule of the fermion mass matrices for up- and down-type quark mass matrices, M_u and M_d , charged lepton mass

matrix, M_e , Dirac neutrino mass matrix, M_ν^D , right-handed neutrino mass matrix, M_R , and left-handed neutrino mass matrix, M_L . Using the sum rule, the prediction of neutrino oscillation parameters has been discussed by inputting the quark masses and mixings. In addition to the accuracy of the charged lepton masses, the measurements of the neutrino mixings are now more accurate rather than the quark masses and mixings, and thus, it is more useful to express the sum rule by inputting the parameters in lepton sector. In this paper, thus, we describe the sum rule in terms of the charged lepton mass matrix M_e and seesaw neutrino mass matrix \mathcal{M}_ν as inputs, and express the quark mass matrices by them. In fact, the quark masses and mixings can receive large radiative corrections at low energy threshold in supersymmetric version of the model, and there can be large ambiguity in the quark sector, compared to the masses and mixing parameters in the lepton sector. Therefore, it is more essential to investigate the properties of the solution inputting the parameters in the lepton sector.

The scale of $\mathbf{126} + \overline{\mathbf{126}}$ vevs, v_R , is important for the breaking the rank-5 $SO(10)$ symmetry down to the rank-4 SM gauge symmetry. The scale is also important to how the light neutrino mass is generated by seesaw mechanism [13]. In the $SO(10)$ model with $\overline{\mathbf{126}}$ coupling, not only the right-handed neutrino Majorana mass for type I seesaw, but also the $SU(2)_L$ triplet contribution to the light neutrino mass is generated, which is known as type II seesaw [14]. In GUT models, an intermediate scale often appears, and it can implement the proper size of the light neutrino masses. However, if v_R is about 10^{13} GeV in SUSY models, the decomposed representations in $\mathbf{126} + \overline{\mathbf{126}}$ lie around the scale, and they are harmful for the gauge coupling evolution since gauge couplings may blow up before the unification. Being motivated by this fact, we feature the solutions for v_R being around 10^{16} GeV. In order to construct the solutions in which the type I seesaw part contributes the neutrino masses, the Yukawa coupling matrix f for $\overline{\mathbf{126}}$ Higgs coupling should be nearly singular and the elements of f^{-1} are enlarged. Such a situation is not obvious if the quark masses and mixings are inputs. Contrary to the situation, in our expression in terms of the parameters in lepton sector, it is easy to decode the structure of the singular matrix.

Using the expression by inputting the parameters in lepton sector, we perform the χ^2 analysis for fitting the quark masses and mixings. As was reported in Refs.[12, 15], the best fit is obtained when $v_R \sim 10^{13}$ GeV. In the analyses in the literatures, the neutrino 13-mixing angle was not fully measured yet. The minimal $SO(10)$ model has predicted that the 13-mixing angle is not too small, and the prediction of the mixing is consistent with the measured value. In fact, even if we change the value of the 13-mixing angle within the experimental 3σ errors, the χ^2 values for the quark masses and mixings do not change very much. Rather, the χ^2 value is more sensitive to the 23-mixing for the atmospheric neutrino oscillation. We show the results of the χ^2 fit by changing of v_R , and also show the result of type I seesaw, where $SU(2)_L$ triplet contribution is negligible. The CP phase in the Pontecorvo-Maki-Nakagawa-Sakata (PMNS) neutrino mixing matrix (PMNS phase) is being measured, and the preferable

region is being obtained by the global data analysis for the neutrino oscillation [16, 17]. We show the implication of the PMNS phase from the χ^2 analysis in the minimal $SO(10)$ model.

As mentioned, the scale v_R is important to how the light neutrino mass is generated by the seesaw mechanism. Footprinting analysis is applicable by investigating the lepton flavor violation (LFV) in SUSY version of the model. In the minimal $SO(10)$ model, the Dirac neutrino coupling and the Majorana neutrino mass matrix are predictable depending on v_R . This feature can impact on the flavor violation in lepton sector in SUSY model, which can cause LFV processes, $\tau \rightarrow \mu\gamma$, $\tau \rightarrow e\gamma$ and $\mu \rightarrow e\gamma$. The source of the flavor violation in the model is (1) Dirac neutrino coupling, $\ell\nu^c H_u$, (2) Majorana coupling, $\ell\ell\Delta_L$, (3) the right-handed charged lepton couplings, $e^c e^c \Delta_R^{--}$, $e^c \nu^c \Delta_R^-$. The first contribution is predictable in the minimal $SO(10)$ model, but the other two depends on the vacua, and thus, they are less predictable. The third one is directly related with the scale v_R and if $v_R \ll O(10^{16})$ GeV, the contribution to the lepton flavor violation can become large, and thus, it can be a probe of the scale v_R in the model. In type II seesaw, the second contribution can also become large. We will perform the calculation of the branching fraction of $\mu \rightarrow e\gamma$ decay and the electric dipole moment (EDM) of electron, using the prediction from the χ^2 analysis in the model and discuss the v_R dependence of the predictions.

In the minimal SUSY GUTs, it is known that the down quark Yukawa coupling is too large to suppress the baryon number violating nucleon decay amplitudes well. In the scheme of the χ^2 analysis of the minimal $SO(10)$ model, it is more precise to say that the holomorphic Yukawa coupling of the down quark is the prediction of the model (inputting the lepton sector parameters). The correction from the low energy SUSY threshold is unknown. In fact, the χ^2 analysis tends to imply that the the down quark mass is less than the lattice calculation from the experimental measurements. We describe the possible SUSY threshold correction, and discuss the proton decay contribution, as well as its relation with other observables.

This paper is organized as follows: In section 2, we introduce the sum rule of the fermion mass matrices in the $SO(10)$ model with the minimal Yukawa interaction, and derive the expression of quark mass matrices in terms of the mass and mixing parameters in the lepton sector. In section 3, we examine the properties of the solutions expressed by the parameters in the lepton sector, and study the v_R dependence of the solutions. The parametrization used in our χ^2 analyses is given in Section 4. In section 5, the method of the χ^2 fits is described, and the results of which are shown in section 6. The predictions of the phase in neutrino oscillations are illustrated in section 7. In section 8, we apply our fit results to the calculations of branching ratio of $\mu \rightarrow e\gamma$ process. We also mention the v_R dependence of the results and study the importance to calculate the electron EDM. The proton decay amplitudes which have to be suppressed to satisfy the current experimental bounds are studied in section 9. In section 10, we discuss the possible modification of the Yukawa couplings by the SUSY threshold corrections. Section 11 is devoted to conclusions and discussions. In Appendix,

we express the square root matrix, which is necessary to express the solution in terms of the parameters of the lepton sector.

2 Sum rule of the fermion mass matrices in the minimal $SO(10)$ model

The minimal $SO(10)$ model¹ is defined as that in which the Yukawa interaction is minimal, namely, only $H : \mathbf{10}$ and $\bar{\Delta} : \overline{\mathbf{126}}$ Higgs representations couple to the fermions $\psi : \mathbf{16}$ by renormalizable interaction:

$$W_Y = \frac{1}{2} \mathbf{h}_{ij} \psi_i \psi_j H + \frac{1}{2} \mathbf{f}_{ij} \psi_i \psi_j \bar{\Delta}. \quad (2.1)$$

Due to the $SO(10)$ algebra, the coupling matrices are symmetric, $\mathbf{h}_{ij} = \mathbf{h}_{ji}$ and $\mathbf{f}_{ij} = \mathbf{f}_{ji}$.

The Yukawa coupling (after $SO(10)$ symmetry is broken down to SM) is given as follows:

$$\begin{aligned} Y_u &= h + r_2 f, \\ Y_d &= r_1 (h + f), \\ Y_e &= r_1 (h - 3f), \\ Y_\nu &= h - 3r_2 f, \end{aligned} \quad (2.2)$$

where r_1 and r_2 depend on the Higgs mixing (doublet Higgs mixing in $\mathbf{10}$ and $\overline{\mathbf{126}}$), and h and f are original Yukawa matrices \mathbf{h} and \mathbf{f} multiplied by Higgs mixings²:

$$h = V_{11} \mathbf{h}, \quad f = \frac{U_{12}}{\sqrt{3}r_1} \mathbf{f}, \quad r_1 = \frac{U_{11}}{V_{11}}, \quad r_2 = r_1 \frac{V_{13}}{U_{12}}. \quad (2.4)$$

¹ In this paper, we define the minimality of the $SO(10)$ model on the Yukawa interaction: The matter representations couple to only $\mathbf{10}$ and $\overline{\mathbf{126}}$ Higgs representations, and the number of parameters in the Yukawa couplings is minimal (without a symmetry). People often impose the minimality of the model even on the Higgs contents, $\mathbf{10} + \overline{\mathbf{126}} + \mathbf{126} + \mathbf{210}$, in which the number of parameters in the Higgs interactions is minimal (in addition to the minimality in the Yukawa interactions). In this case, however, the SUSY version of the model suffers some delicate mismatches between all the fermion data fittings appeared in the recently developed measurements and the self-consistency of the gauge coupling unification [15], and the framework suggests a non-SUSY model (or split SUSY) [18, 19]. Since we focus on the prediction on the Yukawa structure which can communicate with the low energy phenomena, we impose the minimality just on the Yukawa interactions. See section 11 for discussion.

² The unitary matrices U and V are the diagonalizing matrices of the doublet Higgs matrix M_{doublet} : $UM_{\text{doublet}}V^T$ is diagonal,

$$-\mathcal{L}_{\text{doublet}} = (H_d^{10}, \bar{\Delta}_d, \Delta_d, \Phi_d) M_{\text{doublet}} (H_u^{10}, \Delta_u, \bar{\Delta}_u, \Phi_u)^T. \quad (2.3)$$

The lightest linear combinations of the doublets will be the MSSM Higgs doublets. The detail can be found in Ref.[20] (and [9] in different conventions).

The charged fermion masses are obtained as

$$M_u = Y_u v_u, \quad M_d = Y_d v_d, \quad M_e = Y_e v_d, \quad M_\nu^D = Y_\nu v_u. \quad (2.5)$$

where v_u and v_d are the VEVs of up- and down-type Higgs fields. We obtain the relation of the mass matrices as

$$M_d = M_e + \frac{4}{1-r_2} F = r M_u + F, \quad (2.6)$$

$$r M_\nu^D = M_e + 3F, \quad (2.7)$$

where

$$r = r_1 \frac{v_d}{v_u} \equiv r_1 \cot \beta, \quad (2.8)$$

and the matrix F , which is proportional to the $\overline{\mathbf{126}}$ Higgs coupling matrix, is

$$F = r(1-r_2) f v_u. \quad (2.9)$$

Roughly, we obtain $r \sim m_b/m_t$.

The right-handed Majorana neutrino mass matrix is obtained as

$$M_R = \sqrt{2} \mathbf{f} v_R, \quad (2.10)$$

where v_R is a VEV of $\overline{\mathbf{126}}$. Practically, we denote

$$M_R = c_R v_R f, \quad (2.11)$$

where

$$c_R = \sqrt{6} \frac{r_1}{U_{12}} = \sqrt{6} \frac{r_2}{V_{13}}, \quad (2.12)$$

for the current Notation. Because U_{12} and V_{13} are components of the diagonalization unitary matrix for doublet Higgs fields, c_R has a minimal value. The size of c_R is related to the size of original \mathbf{f} coupling. It will be important to derive the GUT scale threshold correction for flavor violation. One can rewrite as

$$M_R = \frac{c_R v_R}{r(1-r_2) v_u} F. \quad (2.13)$$

We note here that the $SO(10)$ breaking vacuum can be specified by one complex parameter for the Higgs contents: $\mathbf{10} + \mathbf{126} + \overline{\mathbf{126}} + \mathbf{210}$ [8, 9]. The coefficient r_2 is determined by the complex parameter³. For typical examples, $r_2 = 1$ for a left-right symmetry vacuum, $r_2 = 0$

³ This is one of the reason why the model with minimal number of Higgs multiplets in the Higgs potential does not provide a solution which can agree with observation in the minimal SUSY version of the minimal $SO(10)$ [15].

for flipped- $SU(5)$ vacuum, and $r_2 = \infty$ for $SU(5)$ vacuum (more precisely $U_{12} = 0$, and therefore, $f = 0$ and $r_2 f$ is finite). In Pati-Salam vacuum, $V_{13} = U_{12} = 0$.

The seesaw neutrino mass matrix can be written as [13, 14]

$$\mathcal{M}_\nu = M_L - M_\nu^D M_R^{-1} (M_\nu^D)^T, \quad (2.14)$$

where M_L is the left-handed neutrino Majorana mass which comes from $SU(2)_L$ triplet coupling [21], $\ell\ell\Delta_L$. In $SO(10)$ model, the $\overline{\mathbf{126}}$ Higgs also includes the $SU(2)_L$ triplet Δ_L and the Yukawa coupling generates both M_L and M_R . Therefore, M_L is also proportional to the coupling matrix f and we denote

$$M_L = c_L v_L f. \quad (2.15)$$

In the $SO(10)$ model, if there is $\mathbf{210}$ or $\mathbf{54}$ Higgs representation⁴, the VEV of Δ_L , $\langle\Delta_L\rangle = v_L$, can be obtained as $v_{\text{weak}}^2/M_\Delta$, where M_Δ is the mass of the $SU(2)_L$ triplet.

For convenience, we reparameterize M_R and M_L as

$$M_R = \frac{1}{r^2 R} F \times 10^{10}, \quad (2.16)$$

$$M_L = \delta F \times 10^{-10}, \quad (2.17)$$

where

$$R \equiv \frac{1-r_2}{r} \frac{v_u}{c_R v_R} \times 10^{10}, \quad \delta \equiv \frac{c_L v_L}{r(1-r_2)v_u} \times 10^{10}. \quad (2.18)$$

The factor 10^{10} is attached for a numerical convenience. We will treat R as a parameter to specify the scale of v_R implicitly. For example, if $v_R \sim 10^{13}$ GeV, one obtains $R \sim O(1)$ roughly. For $v_R \sim 10^{16}$ GeV, one finds $R \sim O(10^{-3})$.

Using the relation, $rM_\nu^D = M_e + 3F$, we obtain

$$\begin{aligned} \mathcal{M}_\nu \times 10^{10} &= (\delta F - R(M_e + 3F)F^{-1}(M_e + 3F)) \\ &= ((\delta - 9R)F - 6RM_e - RM_e F^{-1}M_e). \end{aligned} \quad (2.19)$$

This can be rewritten as a quadratic equation in terms of $M_e^{-1/2} F M_e^{-1/2}$, and we obtain

$$F = \frac{1}{18R - 2\delta} M_e^{1/2} \left(K - 6R\mathbf{1} + \sqrt{K^2 - 12RK + 4\delta R\mathbf{1}} \right) M_e^{1/2}, \quad (2.20)$$

where

$$K \equiv -M_e^{-1/2} \hat{\mathcal{M}}_\nu M_e^{-1/2}, \quad \hat{\mathcal{M}}_\nu \equiv \mathcal{M}_\nu \times 10^{10}. \quad (2.21)$$

The square root matrix is defined in the Appendix. Using the expression of F matrix, the quark mass matrices, M_u and M_d , can be given as a function of charged lepton mass matrix M_e and the light neutrino mass matrix \mathcal{M}_ν .

⁴ When $\mathbf{54}$ is employed to generate the triplet contribution to the neutrino masses [22], the $SO(10)$ breaking vacua is modified, and r_2 parameter can be independent to the vacua.

3 Property of the solution by inputting the lepton parameters

We examine how the solution with $c_{R\nu R} \sim O(10^{16})$ GeV is obtained, and we study the property of the solution. One may think that the 0.05 eV neutrino mass can be easily obtained even if $c_{R\nu R} \sim 10^{16}$ GeV because the scale of $M_R = c_{R\nu R}f$ can be naturally $O(10^{14})$ GeV for the component of f to be $O(10^{-2})$. However, such a naive thought is true only if the atmospheric mixing is small. In fact, in order to reproduce a large atmospheric mixing, not only $(\mathcal{M}_\nu)_{33}$ but also $(\mathcal{M}_\nu)_{23}$ should be $O(0.01)$ eV. In the M_e -diagonal basis, one obtains $(M_e F^{-1} M_e)_{23} \ll (M_e F^{-1} M_e)_{33}$, and thus, to obtain a large 23-mixing, one needs a cancellation in (3,3) element of \mathcal{M}_ν , and the naive thought above does not work.

To obtain the large atmospheric mixing, $(M_e f^{-1} M_e)_{23}/(c_{R\nu R})$ has to be $O(0.01)$ eV. Because the size of f is $O(0.01)$ due to the fitting of quark masses and mixings, the naive size of the $c_{R\nu R}$ is $O(10^{13}) - O(10^{14})$ GeV, which corresponds to $R \sim O(1)$. One can find a solution for $c_{R\nu R} \sim O(10^{16})$ GeV (i.e. $R \sim 10^{-3}$), only if the matrix f is nearly singular and f^{-1} is enhanced (compared to its naive size from each component).

We note that the solution for the nearly singular f matrix is also found in Ref.[15] (they call the solution as ‘‘Mixed’’). However, if one fits the charged fermion masses, there is no reason that f is close to a singular matrix, and it is not easy to study the property of the solution. We describe the neutrino mass and mixing parameters to be inputs, and construct a solution where the situation of small $\det f$ can be seen explicitly. Even if we apart from the minimal model, the solution of nearly singular M_R matrix should be investigated. We believe that the description of nearly singular M_R is useful to study how the light neutrino mass scale is obtained in seesaw models.

As obtained in the previous section, the matrix F is expressed as in Eq.(2.20). Now, by using the formula given in Appendix, let us express the matrix

$$K - 6R\mathbf{1} + \sqrt{(K - 6R\mathbf{1})^2 + D\mathbf{1}}, \quad (3.1)$$

where $D \equiv 4\delta R - 36R^2$. Surely because K and $(K - 6R\mathbf{1})^2 + D\mathbf{1}$ can be diagonalized simultaneously, we can easily obtain

$$K - 6R\mathbf{1} + \sqrt{(K - 6R\mathbf{1})^2 + D\mathbf{1}} = \sum_i \left(\lambda_i - 6R + s_i \sqrt{(\lambda_i - 6R)^2 + D} \right) \Lambda_i, \quad (3.2)$$

where λ_i ($i = 1, 2, 3$) are eigenvalues of matrix K , s_i are signs for the square roots, and Λ_i are given in Appendix. By the definition of the matrix K , $K = -M_e^{-1/2} \hat{\mathcal{M}}_\nu M_e^{-1/2}$ (where $\hat{\mathcal{M}}_\nu = \mathcal{M}_\nu \times 10^{10}$), we obtain

$$M_e^{1/2} \Lambda_1 M_e^{1/2} = \frac{1}{(\lambda_1 - \lambda_2)(\lambda_1 - \lambda_3)} \left(\hat{\mathcal{M}}_\nu M_e^{-1} \hat{\mathcal{M}}_\nu + (\lambda_2 + \lambda_3) \hat{\mathcal{M}}_\nu + \lambda_2 \lambda_3 M_e \right), \quad (3.3)$$

and similarly for $\Lambda_{2,3}$.

In the limit of $R \rightarrow 0$ (i.e. $c_R v_R \rightarrow \infty$), we obtain

$$F \rightarrow -\frac{1}{2\delta} M_e^{1/2} \left(K + \sqrt{K^2} \right) M_e^{1/2}. \quad (3.4)$$

So, let us evaluate $K + \sqrt{K^2}$. One can write down

$$K + \sqrt{K^2} = V \begin{pmatrix} (1+s_1)\lambda_1 & & \\ & (1+s_2)\lambda_2 & \\ & & (1+s_3)\lambda_3 \end{pmatrix} V^{-1} = \sum_i (1+s_i)\lambda_i \Lambda_i. \quad (3.5)$$

For example, suppose $s_1 = -1$ and $s_{2,3} = 1$ (because the square root of a complex number has two branches, we choose a sign convention $\sqrt{\lambda^2} = \lambda$ to define s_i), one finds

$$K + \sqrt{K^2} = 2 \sum_{i=2,3} \lambda_i \Lambda_i = 2K - 2\lambda_1 \Lambda_1. \quad (3.6)$$

As a result, we obtain under the choice of s_i and in the limit of $R \rightarrow 0$,

$$F = \frac{1}{\delta} \left(\hat{\mathcal{M}}_\nu + \lambda_1 M_e^{1/2} \Lambda_1 M_e^{1/2} \right) \quad (3.7)$$

$$= \frac{1}{\delta} \frac{1}{(\lambda_1 - \lambda_2)(\lambda_1 - \lambda_3)} \left(\lambda_1 \hat{\mathcal{M}}_\nu M_e^{-1} \hat{\mathcal{M}}_\nu + (\lambda_1^2 + \lambda_2 \lambda_3) \hat{\mathcal{M}}_\nu + \lambda_1 \lambda_2 \lambda_3 M_e \right). \quad (3.8)$$

In the choice of $s_1 = -1$, $s_2 = s_3 = 1$, it can be written as

$$K + \sqrt{K^2} = 2V \begin{pmatrix} 0 & & \\ & \lambda_2 & \\ & & \lambda_3 \end{pmatrix} V^{-1}. \quad (3.9)$$

Therefore, $\text{rank}(K + \sqrt{K^2}) = 2$ in this case. As a consequence, one of the right-handed neutrinos is very light compared to the other two because the right-handed Majorana mass matrix is proportional to F . Needless to say, R is finite (though it is small), and therefore, the lightest right-handed neutrino is not massless.

For a choice of $s_1 = s_2 = s_3 = 1$, one obtains

$$K + \sqrt{K^2} = 2K, \quad (3.10)$$

and thus, in the limit of $R \rightarrow 0$,

$$F \rightarrow \frac{1}{\delta} \hat{\mathcal{M}}_\nu. \quad (3.11)$$

Therefore, this choice corresponds to the case where the right-handed neutrinos are decoupled, and the triplet contribution is dominant (namely $\mathcal{M}_\nu = M_L$). It is known that the fits of fermion masses and mixings are not good in the triplet-dominant case [15]. The difference

compared to the previous case comes from the contribution from $\lambda_1 M_e^{1/2} \Lambda_1 M_e^{1/2}$, which makes the fits better. In our description of the solution, the triplet-dominant case is contained in the expression just by a choice of the signs of the square root matrix. In fact, as we execute the χ^2 analysis in the following sections, the triplet-dominant case does not appear in the fits by χ^2 minimum, because it gives a large χ^2 value. Therefore, we call the combination of the triplet and type I seesaw contributions just as type II solution, which is intrinsic in the $SO(10)$ model. In the Ref.[15], they name the solutions as ‘‘Mixed’’ and ‘‘Mixed’’, but those two solutions are continuously connected as a function of the parameter R in our description.

We note that the dependence of R is small in the type II solution for $s_1 = -1, s_2 = s_3 = 1$ for small R (namely, large $c_R v_R$) as one can find from the $R \rightarrow 0$ limit. In type I seesaw ($\delta = 0$), the F matrix in the limit of $R \rightarrow 0$ can be written as

$$F \rightarrow \frac{1}{18R} M_e^{1/2} \left(K + \sqrt{K^2} \right) M_e^{1/2}, \quad (3.12)$$

and it surely depends on R . For the solution $s_1 = s_2 = s_3 = 1$, one obtains

$$F \rightarrow -\frac{1}{9R} \hat{\mathcal{M}}_\nu. \quad (3.13)$$

For a smaller value of R , the component of F becomes large and it is expected that there is no solution. For a choice of $s_1 = s_2 = s_3 = -1$, one obtains⁵

$$F \simeq R M_e^{1/2} K^{-1} M_e^{1/2} = -R M_e \mathcal{M}_\nu^{-1} M_e. \quad (3.15)$$

For $R \rightarrow 0$, F becomes small in this choice and which means there is up-down symmetry ($M_d \propto M_u$) in the limit, and there is no solution. Therefore, there may no solution for $c_R v_R > O(10^{16})$ GeV in type I.

⁵ Because of the algebraic equation $(K - 6R\mathbf{1} + \sqrt{K^2 - 12RK + 4\delta R\mathbf{1}})(K - 6R\mathbf{1} - \sqrt{K^2 - 12RK + 4\delta R\mathbf{1}}) = 2R(18R - 2\delta)\mathbf{1}$, one obtains

$$\begin{aligned} F &= \frac{1}{18R - 2\delta} M_e^{1/2} (K - 6R\mathbf{1} - \sqrt{K^2 - 12RK + 4\delta R\mathbf{1}}) M_e^{1/2} \\ &= 2R M_e^{1/2} (K - 6R\mathbf{1} + \sqrt{K^2 - 12RK + 4\delta R\mathbf{1}})^{-1} M_e^{1/2}. \end{aligned} \quad (3.14)$$

4 Parametrization

The relation is summarized as

$$rM_u = M_e + \frac{3-r_2}{1-r_2}F, \quad (4.1)$$

$$M_d = rM_u + F, \quad (4.2)$$

$$F = \frac{1}{18R-2\delta}M_e^{1/2} \left(K - 6R\mathbf{1} + \sqrt{K^2 - 12RK + 4\delta R\mathbf{1}} \right) M_e^{1/2}, \quad (4.3)$$

$$K = -M_e^{-1/2} \hat{\mathcal{M}}_\nu M_e^{-1/2}. \quad (4.4)$$

We work on the basis where the charged lepton mass matrix M_e is diagonal:

$$M_e = \text{diag.} (m_e e^{i\alpha_e}, m_\mu e^{i\alpha_\mu}, m_\tau e^{i\alpha_\tau}), \quad (4.5)$$

The light neutrino mass matrix is parametrized as

$$\mathcal{M}_\nu = \bar{U} \text{diag.} (m_1 e^{i\alpha_1}, m_2 e^{i\alpha_2}, m_3 e^{i\alpha_3}) \bar{U}^T, \quad (4.6)$$

and the unitary matrix \bar{U} is the PMNS neutrino matrix, and we use the usual convention by particle data group (PDG). In the matrix \bar{U} , there are three neutrino mixing angles $\theta_{12}, \theta_{23}, \theta_{13}$ and a CP phase δ_{PMNS} in neutrino oscillation. As a convention, the mass parameters, $m_e, m_\mu, m_\tau, m_1, m_2, m_3$ are given as real and positive values.

As one can find easily, one of the phases $\alpha_e, \alpha_\mu, \alpha_\tau, \alpha_1, \alpha_2, \alpha_3$ can be made to be zero without loss of generality, since the relation is covariant under

$$M_{u,d,e} \rightarrow e^{i\alpha} M_{u,d,e}, \quad \mathcal{M}_\nu \rightarrow e^{i\alpha} \mathcal{M}_\nu. \quad (4.7)$$

We choose $\alpha_1 = 0$ as a convention. The relation is also covariant under the rephasing:

$$R \rightarrow e^{i\alpha} R, \quad \delta \rightarrow e^{i\alpha} \delta, \quad M_{u,d,e} \rightarrow e^{-i\alpha} M_{u,d,e}, \quad (4.8)$$

and thus we can choose R to be real (and positive) without loss of generality. We can also define the parameter r to be real. Therefore, the parameters in this parametrization are the following:

$$\begin{aligned} & m_e, m_\mu, m_\tau, m_1, m_2, m_3, \\ & \alpha_e, \alpha_\mu, \alpha_\tau, \alpha_2, \alpha_3, \\ & \theta_{12}, \theta_{23}, \theta_{13}, \delta_{\text{PMNS}}, \\ & r_2(\text{complex}), r, \\ & \delta(\text{complex}), R, \end{aligned} \quad (4.9)$$

and there are 21 degrees of freedom in total.

The input parameters in the lepton sector are

$$m_e, m_\mu, m_\tau, \theta_{12}, \theta_{13}, \theta_{23}, \Delta m_{\text{sol}}^2, \Delta m_{\text{atm}}^2, \delta_{\text{PMNS}}, \quad (4.10)$$

and the PMNS phase δ_{PMNS} will be treated as output in our analysis. The parameters in the quark sector are

$$m_u, m_c, m_t, m_d, m_s, m_b, V_{us}, V_{cb}, V_{ub}, \delta_{\text{KM}}, \quad (4.11)$$

which we will fit by using the freedom in the model. Totally, there are 19 degrees for the observables⁶.

Just from the degrees of freedom, one can fit all the 19 parameters using the full degrees of freedom in the model, in principle. However, the parameters we need to fit is hierarchical and some of the degrees are phases, and consequently, the fits do not necessarily done contrary to the simple number counting expectation. Actually, due to the hierarchy $m_u/m_t \ll m_e/m_\tau \ll m_d/m_b$, the complex freedom r_2 should be almost consumed to fit the up-quark mass m_u (roughly, the solution is obeyed by a cubic equation of r_2 , $\det M_u \rightarrow 0$). Thus, roughly speaking, to fit m_u , two degrees of freedom is consumed. As we have explained, the fit does not depend on R for small R very much, and then the phase of δ is not an active freedom due to the rephasing covariance described above. Therefore, the active number of parameters to fit the quark masses and mixings are reduced. As a result, for the case of small R , down-quark mass m_d is not fully fit as we will see later, though $R \sim O(1)$ ($c_R v_R \sim 10^{13}$ GeV) solution in type II can reproduce m_d , as it was known in literature [15].

5 Method of χ^2 fit

Before going to the detailed description of the fit process, we explain the equations to solve the quark masses which we can find quickly from the expression,

$$rM_u = M_e + \frac{3+r_2}{1-r_2}F = M_e^{1/2} \left(\mathbf{1} + \frac{3+r_2}{1-r_2} \frac{K-6R\mathbf{1} + \sqrt{(K-6R\mathbf{1})^2 + D\mathbf{1}}}{18R-2\delta} \right) M_e^{1/2}. \quad (5.1)$$

As we have already noted, due to the hierarchy $m_u/m_t \ll m_e/m_\tau$, the matrix in the bracket in the above equation has to be nearly singular. Therefore,

$$\frac{1-r_2}{3+r_2} + \frac{\lambda_i - 6R + s_i \sqrt{(\lambda_i - 6R)^2 + D}}{18R - 2\delta} \rightarrow 0 \quad (5.2)$$

⁶ Depending on the size of absolute neutrino mass, the neutrino Majorana phases α_2 and α_3 and the neutrino mass m_1 can be the observables in the future by neutrinoless double beta decay and the radiative emission of neutrino pairs from excited atoms [23], but we do not count them as observables in this paper.

Fixed Values			Parameters to fit		
m_u	3.961×10^{-4} GeV	[24]	m_c	0.1930 ± 0.025 GeV	[24]
m_t	71.0883 GeV	[24]	m_d	$(9.316 \pm 3.8) \times 10^{-4}$ GeV	[24]
m_e	3.585×10^{-4} GeV	[24]	m_s	$(1.76702 \pm 0.5) \times 10^{-2}$ GeV	[24]
m_μ	7.5639×10^{-2} GeV	[24]	m_b	(0.9898 ± 0.03) GeV	[24]
m_τ	1.3146 GeV	[24]	V_{us}	0.224 ± 0.002	[25]
Δm_{sol}^2	7.54×10^{-5} eV ²	[17]	V_{cb}	$(3.7 \pm 0.13) \times 10^{-2}$	[25]
Δm_{atm}^2	2.4×10^{-3} eV ²	[17]	V_{ub}	$(3.7 \pm 0.45) \times 10^{-3}$	[25]
θ_{12}	0.583	[17]	δ_{KM}	1.18 ± 0.2	[25]
θ_{23}	0.710, $\pi/4$	[17]			
θ_{13}	0.156	[17]			

Table 1: *The reference parameters used in the fit.*

for one of $i = 1, 2, 3$, where λ_i are eigenvalues of the matrix K as was given previously. By perturbation from the above relation, the up-quark mass m_u can be easily fit. One can also easily solve the equation by r :

$$r^2(m_u^2 + m_c^2 + m_t^2) = r^2 \text{Tr} M_u M_u^\dagger = \text{Tr} \left(M_e + \frac{3 + r_2}{1 - r_2} F \right) \left(M_e + \frac{3 + r_2}{1 - r_2} F \right)^\dagger, \quad (5.3)$$

and thus, roughly speaking, the top quark mass m_t can be easily fit by using r . As we have explained, we will try to fit the masses and mixings in quark sector by inputting the masses and mixings in lepton sector. The parameters to fit are now

$$m_c, m_d, m_s, m_b, V_{us}, V_{cb}, V_{ub}, \delta_{\text{KM}}. \quad (5.4)$$

The χ^2 function is defined as

$$\chi^2 = \sum_i \frac{(\chi_i - \hat{\chi}_i)^2}{\hat{\sigma}_i^2}, \quad (5.5)$$

where $\hat{\chi}_i$ and $\hat{\sigma}_i$ are the experimental measurements of the parameters and their standard deviations of errors.

The values and uncertainties used in the fit are summarized in Table 1 where we use the value of the quark mass in Table III of Ref.[24] (MSSM, $\tan \beta = 10$) and calculate the quark mixing angle and KM phases at GUT scale from PDG data [25] by $\overline{\text{DR}}$ scheme.

For the minimization, we use the Metropolis-Hastings (MH) algorithm [26] of the Markov Chain Monte Carlo (MCMC) method. Since we expect that there exists many local minima, we perform the replica exchange MCMC (REMC) sampling [27] where several copies of the Markov chain with various temperature T_i are simultaneously simulated. Each chain performs MH scheme under a likelihood function defined by $\exp[-\chi^2/(2T_i)]$. Every after performing

some MC steps, the state of the chains are swapped by comparing the values of the likelihood. For ordinary MCMC, the state of the chain is often trapped at a local minimum and costs a large amount of time when we search a likelihood function with many local minima. For REMC, on the other hand, a replica with high temperature (> 1) has a flatter distribution function and the sampling point can easily move on to another local minimum. Thanks to the swapping algorithm, this transition can propagate to low-temperature replicas and therefore we can effectively sweep all the local minima.

We should note, however, that it is still challenging to find the absolute global minimum of the likelihood function with many local deep minima. We have made much effort to find the minimum including changing the initial parameter set, tuning the replica temperatures as well as the width of the parameter jump in MCMC sampling. Nevertheless, there is always a possibility that the likelihood has another better minimum due to our limited hardware and calculation time.

The fits are done assuming that M_L is negligible (type I: $\delta = 0$) or non-negligible (type II: $\delta \neq 0$)⁷ under two values of θ_{23} (0.710, $\pi/4$). In the MCMC, we fix the scale parameter R to precisely investigate the χ^2 behavior against the scale parameter, and therefore, the χ^2 function has seven (nine) free parameters for type I (type II).⁸ We adopt uniform prior for the phases ($\alpha_e, \alpha_\mu, \alpha_\tau, \alpha_2, \alpha_3, \delta_{\text{PMNS}}, \text{Arg}(\delta)$) from $-\pi$ to π and the magnitude of the seesaw parameter $|\delta| \leq 500$. Log flat prior is applied to m_1 over the range of $10 \leq -\log_{10}(m_1/\text{GeV}) \leq 16$.

6 Fit results

Fig. 1 shows R (and $c_{R\nu R}$) dependence of χ^2 values. For all cases, the global best fit is found at around $c_{R\nu R} \sim O(10^{13})$ GeV where the χ^2 value is 1.5–2 for type I and ≤ 0.001 for type II. The χ^2 value of type I mainly stems from down quark mass (~ 0.44 MeV) which is smaller than the experimental value by $\sim 1.2-1.3\sigma$. For type I, another local minimum appears at $c_{R\nu R} \sim O(10^{15})$ GeV where large deviation is given by m_d ($\sim 1.3\sigma$ smaller) and m_s ($\sim 2\sigma$ larger). For type II, the χ^2 curve becomes flat above $c_{R\nu R} \sim O(10^{14})$ GeV and no prominent local minimum exists. As we expected in Section 3, $c_{R\nu R} \sim O(10^{16})$ GeV is disfavored for type I while type II gives a χ^2 value of $\sim 2-2.5$ where the deviation is dominated

⁷ The parameter δ is given in Eq.(2.17), and the classification of the χ^2 minimal solution is described in section 3.

⁸ We also search the global best fit and the fit at $R = 0.001$ allowing the neutrino oscillation parameters ($\theta_{12}, \theta_{13}, \theta_{23}$) and neutrino mass difference ($\Delta m_{\text{sol}}^2, \Delta m_{\text{atm}}^2$) free within a range of 3σ . We find that most of the parameters except for θ_{23} converge around their central values and we decide to fix these reference values.

For θ_{23} , on the other hand, although the θ_{23} deviation does not significantly change the χ^2 values, its uncertainty is still large. Moreover, the θ_{23} value has a correlation with δ_{PMNS} at the χ^2 minimum as one can see in section 7. Therefore, in our fit, we adopt two values of θ_{23} as the reference value, where one is the global fit of the three neutrino oscillation parameters [17] ($\theta_{23} = 0.71$) and the other is the maximal mixing ($\theta_{23} = \pi/4$).

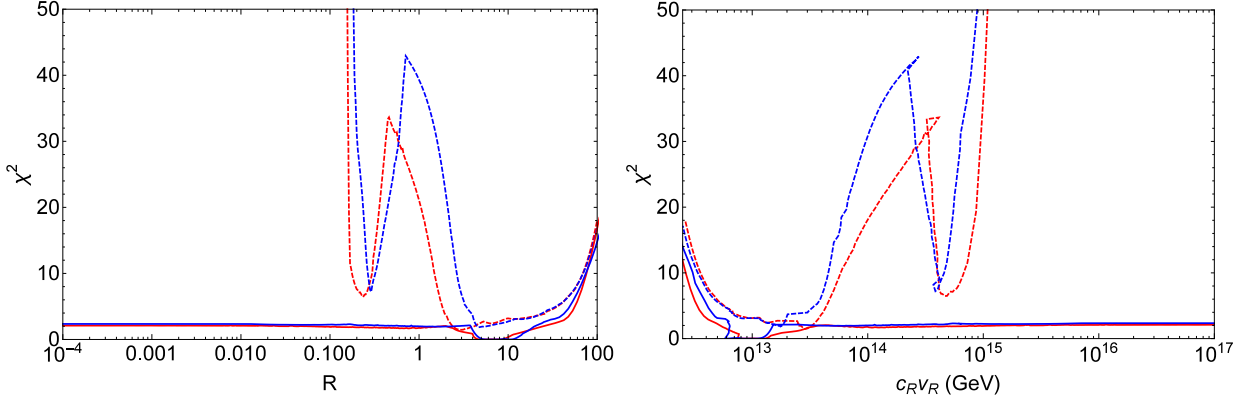


Figure 1: **Left panel:** R dependence of χ^2 for type I of $\theta_{23} = 0.710$ (red dashed line), $\pi/4$ (blue dashed line) and type II of $\theta_{23} = 0.710$ (red solid line), $\pi/4$ (blue solid line). **Right panel:** The same figure as the left one but we transform R to the energy scale $c_R v_R$.

by the down quark mass ($\sim 1.4\sigma$ smaller). Compared with the case of $\theta_{23} = 0.710$, although the difference is not obvious, $\theta_{23} = \pi/4$ gives slightly larger χ^2 values and shifts the minima to lower energy scale. Tables 2 and 3 show the summary of the fit parameters and χ^2 at each global best fit ($c_R v_R \sim O(10^{13})$ GeV), the local minimum of type I ($c_R v_R \sim O(10^{15})$ GeV) and $R = 0.001$ of type II ($c_R v_R \sim O(10^{16})$ GeV).

The numerical quantities of the right-handed neutrino mass are also obtained from the fit. For type II, we find that the sign combination of $\sqrt{K} (s_1, s_2, s_3)$ becomes a permutation of $(-1, 1, 1)$ at a low R region ($R < 0.1$). Thus, as investigated in section 3, the lightest right-handed neutrino mass is small compared with the other two eigenvalues. For example, at $R = 0.001$, the lightest mass is $6.9 (5.5) \times 10^8$ GeV while the other masses are $3.3 (3.5) \times 10^{14}$ GeV and $1.3 (1.2) \times 10^{16}$ GeV for $\theta_{23} = 0.71$ ($\pi/4$). In addition, the lightest right-handed neutrino mass is insensitive to R while the other two eigenvalues of the neutrino mass behave as $\sim 1/R$ in that small R region, which is also consistent with the analytical consideration in section 3. Around the global best fit ($c_R v_R \sim 10^{13}$ GeV), in contrast, the lightest neutrino mass grows and becomes nearly the same scale as the second largest neutrino mass. For example, at the global best fit R , the lightest neutrino mass is $2.4 (2.2) \times 10^{10}$ GeV while other two eigenvalues are $4.6 (3.2) \times 10^{10}$ GeV and $11.1 (6.9) \times 10^{11}$ GeV for $\theta_{23} = 0.71$ ($\pi/4$).

We assume the normal hierarchy of the neutrino masses, $m_1 < m_2 < m_3$, in the above discussion. We also search for χ^2 minimum for the inverted hierarchy case, which can be done since the neutrino mass matrix is given as input in our formula. We find that the fit does not lead to a competitive result within the energy scale from 10^{13} GeV to 10^{16} GeV, which gives $\chi^2 > 200$.

Type I				
	Best fit		Local minimum	
θ_{23}	0.710	$\pi/4$	0.710	$\pi/4$
R	2.9853	4.7315	0.23713	0.29006
α_e	1.2200	-0.15753	0.97741	1.5312
α_μ	-0.77358	1.9305	1.7110	0.95362
α_τ	2.2100	-2.1821	-1.7127	-2.3612
α_2	-2.8818	2.8578	-2.7599	-2.8910
α_3	-0.45528	1.8924	-1.1936	-2.0470
δ_{PMNS}	-0.80638	1.9094	-1.5819	-2.3119
$\log_{10}(m_1/\text{GeV})$	-11.501	-11.273	-11.381	-11.270
m_c (GeV)	0.1955	0.1999	0.2153	0.2098
m_d (GeV)	0.0004810	0.0004270	0.0004380	0.0004416
m_s (GeV)	0.01814	0.01798	0.02705	0.02791
m_b (GeV)	0.9916	0.9885	0.9789	1.004
V_{uc}	0.2242	0.2241	0.2243	0.2245
V_{sb}	0.003703	0.003674	0.004025	0.004011
V_{ub}	0.03692	0.03692	0.03693	0.03612
δ_{KM}	1.218	1.189	1.206	1.190
Pull				
m_c	0.099	0.275	0.893	0.672
m_d	-1.186	-1.328	-1.299	-1.290
m_s	0.094	0.061	1.876	2.048
m_b	0.061	-0.042	-0.362	0.464
V_{uc}	0.086	0.033	0.156	0.229
V_{sb}	0.006	-0.057	0.722	0.691
V_{ub}	-0.065	-0.064	-0.051	-0.675
δ_{KM}	0.190	0.045	0.128	0.048
r	0.0138	0.0144	0.0279	0.0285
r_2	$0.323 + 0.00618i$	$0.311 - 0.00331i$	$2.78 + 0.00190i$	$2.77 - 0.379i$
$c_R v_R$ (GeV)	2.85×10^{13}	1.76×10^{13}	4.69×10^{14}	3.81×10^{14}
χ^2	1.48	1.85	6.70	7.51

Table 2: The fit result for type I. Pull is defined by $(\chi_i - \hat{\chi}_i)/\hat{\sigma}_i$ for each observable.

Type II				
	Best fit		$R = 0.001$	
θ_{23}	0.710	$\pi/4$	0.710	$\pi/4$
R	5.1582	7.2861	0.001	0.001
α_e	-0.81968	-1.8785	-0.66648	-0.25301
α_μ	-1.0015	1.5169	-2.8148	2.8177
α_τ	1.4632	2.8853	-0.53961	-0.84287
α_2	-2.8481	2.8306	-2.8709	-3.1146
α_3	-0.30601	1.1731	-1.9809	-2.8604
δ_{PMNS}	-0.28115	1.4476	-2.3550	-3.1131
$\log_{10}(m_1/\text{GeV})$	-11.592	-11.467	-11.207	-11.173
$ \delta $	75.056	100.11	15.545	16.156
$\text{Arg}(\delta)$	0.11782	0.11535	0.43912	0.51567
m_c (GeV)	0.1931	0.1929	0.1978	0.1989
m_d (GeV)	0.0009278	0.0009309	0.0004138	0.0003936
m_s (GeV)	0.01785	0.01767	0.01980	0.02028
m_b (GeV)	0.9897	0.9898	0.9903	0.9901
V_{uc}	0.2240	0.2240	0.2240	0.2241
V_{sb}	0.003698	0.003698	0.003765	0.003724
V_{ub}	0.03700	0.03699	0.03694	0.03695
δ_{KM}	1.180	1.180	1.195	1.160
Pull				
m_c	0.004	-0.005	0.191	0.236
m_d	-0.010	-0.002	-1.363	-1.416
m_s	0.036	0.000	0.426	0.522
m_b	-0.002	0.000	0.017	0.010
V_{uc}	0.002	-0.012	-0.000	0.027
V_{sb}	-0.005	-0.005	0.144	0.054
V_{ub}	-0.004	-0.009	-0.044	-0.039
δ_{KM}	-0.001	-0.001	0.075	-0.099
r	0.0140	0.0138	0.0230	0.0233
r_2	$0.506 + 0.0252i$	$0.502 + 0.00628i$	$2.15 + 0.227i$	$2.22 - 0.160i$
$c_R v_R$ (GeV)	1.19×10^{13}	0.861×10^{13}	8.86×10^{16}	9.22×10^{16}
χ^2	0.001	0.0003	2.10	2.35

Table 3: *The fit result for type II.*

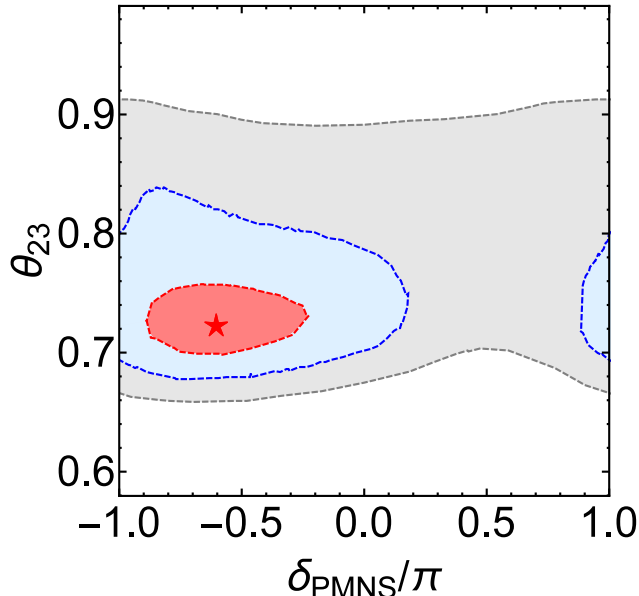


Figure 2: The preferred region of δ_{PMNS} and θ_{23} given by [17]. The best fit is shown by the red star. The red, blue, gray area represents 1σ , 2σ and 3σ region respectively.

7 Prediction of PMNS phase in the neutrino oscillation

The PMNS phase δ_{PMNS} is one of the interesting predictions of our fitting results. Though the accuracy is not still sufficient, the on-going experiments [3] already give a tendency of the parameter region. The long-baseline accelerator experiments and its global fit [28] suggest that θ_{23} larger than $\pi/4$ is slightly favored while the reactor experiments support small $\theta_{23} (< \pi/4)$. Fig. 2 shows the global best fit by [17] which involves both the accelerator and the reactor experiments. Although the wide range of the parameter region is still allowed, negative δ_{PMNS} with small θ_{23} ($< \pi/4$) is slightly favored. It is expected that the experiments will present more accurate δ_{PMNS} as well as θ_{23} within a few years. In addition, accessibility of other future experiments is estimated and found to reach ten and several percent accuracy for θ_{23} and 10 to 40 percent accuracy for δ_{PMNS} [29]. Therefore, it is interesting to compare the current experimental favored region with our fit prediction.

For that purpose, we search for the global χ^2 minimum for each fixed θ_{23} and δ_{PMNS} ⁹ in the range of $0.675 < \theta_{23} < 0.835$ and $|\delta_{\text{PMNS}}| < \pi$ allowing R free within a range of

⁹ One might think that we can construct the same map by simply accumulating the MCMC samples by allowing θ_{23} and δ_{PMNS} free. However, as mentioned in section 5, the χ^2 function has a large number of deep local minimum and it is difficult to explore the detailed χ^2 map under the full free parameter space. Hence, we decide to fix these two parameter for each MCMC simulation.

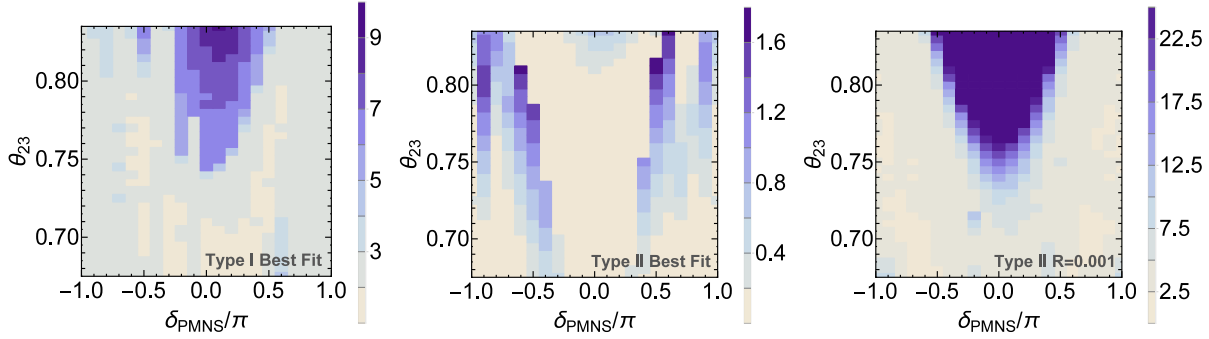


Figure 3: **Left panel:** The χ^2 map of type I global best fit. The colored tiles show the magnitude of χ^2 . **Middle panel:** The χ^2 map of type II global best fit. **Right panel:** The χ^2 map of type II best fit at $R = 0.001$. We set the darkest blue panel to represent $\chi^2 > 25$.

$0.0001 < R < 100$ and also explore the same parameter region at $R = 0.001$ ($c_{R\nu R} \sim 10^{16}$ GeV) for Type II. Here we set the parameter range of θ_{23} as 2σ region of Ref. [17].

Fig. 3 shows the χ^2 map with respect to δ_{PMNS} and θ_{23} for each case. The darker blue region represents higher χ^2 where the step size is given by the color bars beside the map. For type I global best fit (left panel), the figure shows that $|\delta_{\text{PMNS}}/\pi| < 0.3$ is mildly disfavored when θ_{23} is large ($> \pi/4$). The χ^2 value around $|\delta_{\text{PMNS}}/\pi| < 0.3$ gets better as θ_{23} decreases while smaller χ^2 appears at $\delta_{\text{PMNS}}/\pi \sim \pm 0.5$ within a range of $0.71 < \theta_{23} < \pi/4$. For small θ_{23} (< 0.71), $|\delta_{\text{PMNS}}/\pi| < 0.5$ turns out to be a preferred region. Although $\delta_{\text{PMNS}}/\pi \sim -0.3$ with $\theta_{23} \sim 0.675$ gives the lowest χ^2 , a similar χ^2 value is obtained at around $\delta_{\text{PMNS}}/\pi \sim 0-0.4$ with small θ_{23} . At most of the points, the largest contribution to χ^2 comes from (smaller) m_d with $1-2.5\sigma$ deviation. The second largest contribution is from (larger) m_s and (smaller) δ_{KM} , which becomes conspicuous at the disfavored region and reach $1-1.5\sigma$. Interestingly, the χ^2 asymmetry on the δ_{PMNS} sign is mainly derived from the δ_{KM} deviation, the center of which is located at around $\delta_{\text{PMNS}}/\pi \sim 0.1$. If δ_{KM} is more precisely measured in the future, this asymmetry will be stressed, which leads a stronger prediction on the sign of the PMNS phase.

For type II, the χ^2 map of the global best fit (middle panel) shows that χ^2 is small enough under any value of θ_{23} and δ_{PMNS} . In contrast to the type I case, larger χ^2 appears at $|\delta_{\text{PMNS}}/\pi| > 0.5$ in a large θ_{23} (> 0.75) region, implying that the fit becomes an interesting prediction if θ_{23} is large as suggested by the current accelerator experiments. Though a small peak appears at around $|\delta_{\text{PMNS}}/\pi| \sim 0$ when $\theta_{23} > \pi/4$, it is not as prominent as that of the type I case. When θ_{23} is small, on the other hand, most of the points except for $|\delta_{\text{PMNS}}/\pi| \sim \pm 0.4$ gives $\chi^2 < 0.5$ and a better χ^2 value is found at around $|\delta_{\text{PMNS}}/\pi| > 0.5$. Though the χ^2 map is roughly δ_{PMNS} -axis symmetric, the components of the χ^2 value are slightly different with respect to the sign of δ_{PMNS} . In negative δ_{PMNS} region, the largest

contribution to χ^2 is from m_d ($0-1.2\sigma$ smaller) and the second largest contribution is from m_s ($0-0.7\sigma$ smaller) and the other contributions are negligible. When δ_{PMNS} is positive, these contributions become $0-0.8\sigma$ and contributions from δ_{KM} and V_{ub} with $\sim 0.6\sigma$ (larger), $\sim 0.3\sigma$ (larger) also appear at around $|\delta_{\text{PMNS}}/\pi| \sim 0.5$. Here we note that in contrast to the other cases, the m_s deviation is negative when χ^2 is large while it becomes positive at the small χ^2 region around $\delta_{\text{PMNS}} \sim 0$. According to the suggestion given by the accelerator experiments, we also check the χ^2 behavior at large θ_{23} ($0.835 < \theta_{23} < 0.88$) under fixed $\delta_{\text{PMNS}}/\pi = -0.5$ and find that the χ^2 value remains less than 3.0 for all the θ_{23} region. We expect that more accurate measurement against the observables used in our fit will resolve the degeneracy of the χ^2 map in the near future.

For type II of $R = 0.001$ (right panel), though the shape of the χ^2 map is similar to the type I best fit, it seems more symmetric with δ_{PMNS} -axis and its disfavored region is more obvious. The χ^2 value within $|\delta_{\text{PMNS}}/\pi| < 0.5$ steeply increases as θ_{23} becomes large and reaches ~ 80 at $\delta_{\text{PMNS}}/\pi \sim 0$. (In the figure, we set the darkest blue panel to represent $\chi^2 > 25$.) Particularly, $\delta_{\text{PMNS}}/\pi \sim -0.5$ with a large θ_{23} (> 0.81) suggested by the current accelerator experiments is strongly disfavored in this phenomenologically preferred case. Stronger upper bound on θ_{23} can be found when $|\delta_{\text{PMNS}}|$ is small and reaches $\theta_{23} < 0.73$ at $|\delta_{\text{PMNS}}/\pi| \sim 0$. At a point with a small χ^2 (< 5) in our map, the largest contribution to χ^2 comes from m_d ($1-1.5\sigma$ smaller) and m_s ($0-1.5\sigma$ larger). While the m_d contribution does not strongly depend on θ_{23} , δ_{PMNS} , the m_s deviation becomes large at the disfavored region ($|\delta_{\text{PMNS}}/\pi| < 0.5$ with a large θ_{23}) and reaches $\sim 2.5\sigma$. Still, these contributions are subdominant at the disfavored region in which (larger) m_c and (smaller) δ_{KM} give $4-6\sigma$ and $3-4.5\sigma$ deviations, respectively. In addition, (larger) m_b and (larger) V_{ub} also contribute to χ^2 with $3-4\sigma$ deviation around $|\delta_{\text{PMNS}}/\pi| \sim 0$ at a large θ_{23} ($> \pi/4$). Similar to the type I case, the δ_{KM} deviation is slightly δ_{PMNS} -axis asymmetric, which is centered at $|\delta_{\text{PMNS}}/\pi| \sim 0.1$. However, this asymmetry is canceled by the contribution from m_c , m_b which are located at around $|\delta_{\text{PMNS}}/\pi| \sim -0.1$. Hence, we cannot conclude which sign of δ_{PMNS} is preferred only from our fit.

Even though it is not easy to explain how the prediction of the phase is obtained explicitly, one can understand the results qualitatively, especially in the case of $R = 0.001$ for type II. Relating to the result that the fit of the down quark mass is smaller than the observation, (1,1) and (1,2) elements of \mathcal{M}_ν are smaller than the other elements in the fit result. In fact, in the special case with two-zero texture of the neutrino mass matrix, $(\mathcal{M}_\nu)_{11} = (\mathcal{M}_\nu)_{12} = 0$, one obtains a relation among the mixing angles, mass squared ratio, and PMNS phase [30]. Under the two-zero texture assumption, we obtain [31, 32]

$$\cos \delta_{\text{PMNS}} = \frac{\frac{\Delta m_{\text{sol}}^2}{\Delta m_{\text{atm}}^2} \cos 2\theta_{13} \sin^2 2\theta_{12} - 4 \sin^2 \theta_{13} \left(\frac{\Delta m_{\text{sol}}^2}{\Delta m_{\text{atm}}^2} \cos^4 \theta_{12} + \cos 2\theta_{12} \right) \tan^2 \theta_{23}}{4 \sin^3 \theta_{13} \left(1 + \frac{\Delta m_{\text{sol}}^2}{\Delta m_{\text{atm}}^2} \cos^2 \theta_{12} \right) \sin 2\theta_{12} \tan \theta_{23}}. \quad (7.1)$$

In Fig.4, we plot the relation between δ_{PMNS} and θ_{23} in the assumption. Surely, those two

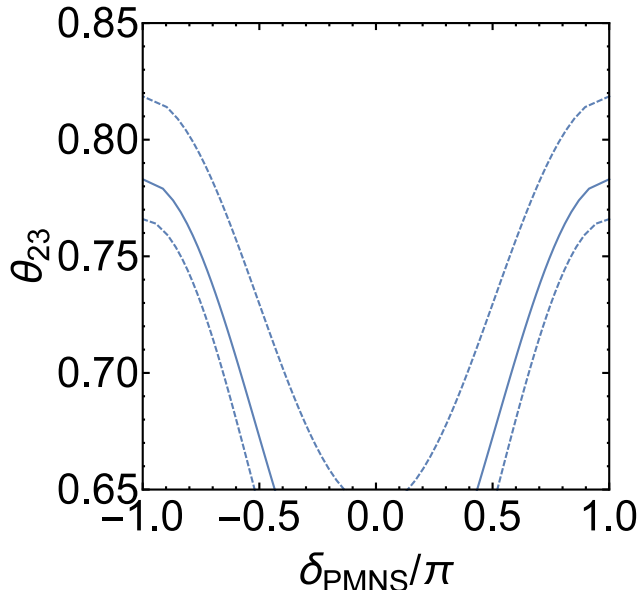


Figure 4: *The relation between δ_{PMNS} and θ_{23} under the two-zero texture assumption: $(\mathcal{M}_\nu)_{11} = (\mathcal{M}_\nu)_{12} = 0$. The solid line is drawn using the center value of θ_{13} : $\sin \theta_{13} = 0.156$, and the dashed lines are drawn to present the 2σ range of θ_{13} . For the mass squared difference and θ_{12} , we use the center values of the global analysis [17].*

elements are not exactly zero in the fits, and the relation provide a guide to understand the fit results for the prediction of the PMNS phase depending on the mixing angle. In fact, the points far from the two-zero texture, such as $(\delta_{\text{PMNS}}, \theta_{23}) \sim (0, 0.8)$, are disfavored in our fits in the case of $R = 0.001$ for type II. There is also such a tendency in the fits in type I, though the detail of the fits is more complicate. In the type II global best fit, on the other hand, the (1,1) and (1,2) elements are not small for the observed values to be tuned. Therefore, the χ^2 values become slightly larger near the points from the two-zero texture. We remark that the smallness of (1,1) and (1,2) elements relates to the suppression of the proton decay amplitudes as we will see later. It is important to measure the PMNS phase and the 23-mixing angle accurately by the long-baseline neutrino oscillation experiments in order to survey the structure of the Yukawa matrices in the $SO(10)$ model.

8 Application to the lepton flavor violation

The fitting of the fermion masses and mixings in the minimal $SO(10)$ model fixes the matrices of the Yukawa couplings. The most interesting application of this feature is to calculate the flavor violation in the SUSY model. In fact, the Dirac and Majorana neutrino mass

matrices are determined (as a function of v_R scale), and the flavor violation is predictable. The importance of the scale v_R can be also illustrated in the whole picture of the flavor violation source in the scheme of the minimal flavor violation assumption. In this section, as an application of the solution of the mass and mixing fitting, we perform the calculation of lepton flavor violation of $\mu \rightarrow e\gamma$ process by assuming the minimal flavor violation, which can be a major sensitive probe to find a footprint.

There are two kinds of amplitudes of $\mu \rightarrow e\gamma$ decay, $A_L : \mu_R \rightarrow e_L\gamma$ and $A_R : \mu_L \rightarrow e_R\gamma$, and the branching fraction of $\mu \rightarrow e\gamma$ is

$$\text{Br}(\mu \rightarrow e\gamma) \propto |A_L|^2 + |A_R|^2. \quad (8.1)$$

Roughly speaking, A_L arises from the chargino loop contribution and the off-diagonal elements in the left-handed slepton mass matrix contribute to it. The right-handed amplitude arises from neutralino loop diagrams : (1) Bino-Higgsino diagram, (2) Bino-Bino diagram. The off-diagonal elements in the right-handed charged lepton mass matrix contribute to the diagram (1), and those of both left- and right-handed slepton mass matrices can contribute to the diagram (2).

The sources of the flavor violation are the following:

1. Dirac Yukawa coupling, $\ell\nu^c H_u$.

The right-handed neutrino ν^c and the Higgs doublet H_u propagate in the loop, and the off-diagonal elements of the left-handed slepton mass matrix are generated [33]. In the minimal $SO(10)$ model, the Dirac neutrino Yukawa coupling and the heaviest right-handed neutrino mass are determined (irrespective of v_R), and thus, this contribution is predictable.

2. Majorana coupling, $\ell\ell\Delta_L$.

The $SU(2)_L$ triplet Δ_L and the left-handed lepton doublet ℓ propagate in the loop, and the off-diagonal elements of the left-handed slepton mass matrix are generated. In the triplet seesaw, when the $SU(2)_L$ triplet contribution is in the sub-eV range, the mass of the Δ_L is about 10^{13} GeV, and this contribution will be important to the lepton flavor violation. Since the coupling matrix is unified to the $\overline{\mathbf{126}}$ Higgs coupling, the Majorana coupling matrix is determined by the fermion mass and mixing fitting, up to the overall mixing parameter. The coupling matrix f is obtained as the original matrix \mathbf{f} multiplied by the Higgs mixing as given in section 2, and thus, this contribution is not fully determined by the fit of the fermion masses and mixings. Since the matrix is obtained up to the overall factor, the ratio of the contributions to $\mu \rightarrow e\gamma$, $\tau \rightarrow \mu\gamma$ and $\tau \rightarrow e\gamma$ is predictable if the contributions from the other sources are small. Because the Higgs mixing cannot be larger than 1, the matrix elements of the Majorana coupling

have lower bounds in the simplest model. However, if the **54** Higgs is adopted, the $SU(2)_L$ triplet from the $\overline{\mathbf{126}}$ is mixed with the one in **54**, and then, the $SU(2)_L$ triplet mixing is also multiplied, and the lower bound from this source is model-dependent.

3. $e^c e^c \Delta_R^{--}$, $e^c \nu^c \Delta_R^-$ couplings.

If the $SU(2)_R$ symmetry or $U(1)_R \times U(1)_{B-L}$ symmetry is broken much below the GUT scale, the fields of Δ_R^{--} and/or Δ_R^- can be light and they propagate in the loop and the off-diagonal elements of the right-handed charged-lepton mass matrix is generated. This contribution is related to the Higgs spectrum and model-dependent, and thus, it is not very predictable. However, if v_R is $\sim O(10^{13})$ GeV, this contribution is not small and need to be considered. Since it contributes to the FCNC from the right-handed sleptons, flavor violating decay is generated from the neutralino loop diagram.

4. $e^c u^c H_C$ coupling.

In the language of $SU(5)$ GUT, $\mathbf{10} \cdot \mathbf{10} \cdot \mathbf{5}_H$ includes this coupling. The right-handed up-type quarks and the colored Higgs fields H_C propagate in the loop, and the off-diagonal elements of the right-handed charged-lepton mass matrix are generated. In the other sources, the mass of the fields which propagate in the loop is supposed to be of the order of 10^{13} GeV, while the colored Higgs mass is $O(10^{16})$ GeV, and thus, this contribution is not very important, compared to the others in the current context of $SO(10)$ model.

In general, those Yukawa coupling Y_{ij} to the charged-leptons can induce off-diagonal elements in the slepton mass matrices by RGE in the form of

$$(M_{\tilde{\ell}, \tilde{e}}^2)_{i \neq j} = -\frac{C}{8\pi^2} \sum_k Y_{ik} Y_{jk}^* (3m_0^2 + A_0^2) \ln \frac{M_*}{M_X}. \quad (8.2)$$

Here m_0 is a universal scalar mass, A_0 is a universal scalar trilinear coupling, M_* is a cutoff scale, M_X is the mass of a heavy field which propagate in the loop, and C is a group weight factor. In particular, the off-diagonal elements induced by the Dirac neutrino Yukawa coupling Y_ν can be roughly written as

$$(M_{\tilde{\ell}}^2)_{i \neq j} = -\frac{1}{8\pi^2} \sum_k (Y_\nu)_{ik} (Y_\nu)_{jk}^* (3m_0^2 + A_0^2) \ln \frac{M_*}{M_{R_k}}, \quad (8.3)$$

where Y_ν is given in the basis where the right-handed neutrino mass matrix is diagonal, and M_{R_k} is an eigenmass of k -th generation right-handed neutrino. It is important to note that the gluino and squark masses should be heavy due to the LHC results, and thus, the amount of the induced FCNC becomes less in the universal SUSY breaking models. The discovery of the 125 GeV Higgs boson also pushes up the squark masses. If the mass of the squarks and gluino are $O(10)$ TeV, it is hard to extract the off-diagonal elements from the flavor data. However,

if the squark and gluino masses are about 2 TeV, the scalar trilinear coupling A_0 has to be large (~ 5 TeV) to obtain the Higgs mass to be 125 GeV, and then, the off-diagonal elements are generated (even if m_0 is small) and the FCNCs are induced slightly. Therefore, the SUSY contribution can be consistent with the experimental results of many of the FCNC processes, but a slight excess can be observed in a process whose amplitude can have an enhancement factor. We remark that the circumstances are changed from the literatures a few years ago.

Other main circumstance changed by the LHC experiments is the SUSY mass spectrum: The gluino and squark masses are bounded from below. The observation of $B_s \rightarrow \mu^+ \mu^-$ to be consistent with the SM prediction also bounds the parameters [34]. Though the bound of the slepton masses, which is important for the lepton flavor violating decays, is not directly related to the gluino and squark mass bound, the slepton masses depend on the gluino and squark mass bounds if the universal SUSY breaking is assumed. The bounds depend on the SUSY breaking scenario. Since the anomaly mediation is an infrared phenomenon, the slepton spectrum is still less bounded compared to the squark masses, even in the GUT models¹⁰. We calculate the lepton flavor violation using the Yukawa couplings by fitting the fermion masses and mixings in the minimal $SO(10)$ model assuming the universality to make the number of SUSY breaking parameters less, and thus, the slepton mass spectrum depends on the gluino mass bound indirectly. We choose the unified gaugino mass $m_{1/2} = 800$ GeV to satisfy the current gluino bound and to be covered the next run at the LHC. We vary the universal scalar mass m_0 , which is important to the slepton masses. The scalar trilinear coupling A_0 is chosen to make the Higgs mass to be 125 GeV, depending on m_0 . The ratio of the vev of up- and down-type Higgs bosons, $\tan \beta$, is an important parameter because the decay width of $\mu \rightarrow e \gamma$ is roughly proportional to $\tan^2 \beta$. We choose $\tan \beta = 10$ in the calculation.

We show the results of the numerical calculation in four cases given by the χ^2 minimum fits, where the right-handed neutrino masses and the Dirac neutrino Yukawa couplings are given as follows in the basis where the charged lepton and the right-handed neutrino mass matrices are real/positive diagonal. Using unphysical phase freedom in SM, we make the $(i, 1)$ components to be real.

1. type II, $c_R v_R = 8.86 \times 10^{16}$ GeV ($R = 0.001$)

$$M_{R_1} = 6.9 \times 10^8 \text{ GeV}, \quad M_{R_2} = 3.3 \times 10^{14} \text{ GeV}, \quad M_{R_3} = 1.2 \times 10^{16} \text{ GeV}, \quad (8.4)$$

$$Y_\nu = \begin{pmatrix} 0.000111 & 0.000203 + 0.000217 i & 0.00888 + 0.00372 i \\ 0.000440 & 0.0308 - 0.0248 i & 0.0426 + 0.0013 i \\ 0.00607 & -0.0276 - 0.0069 i & 0.990 - 0.278 i \end{pmatrix}, \quad (8.5)$$

¹⁰ In fact, if we take the known anomaly of the muon $g-2$ seriously, the universal SUSY breaking is not very favored after the LHC results bound the gluino and squark masses, and the mixed modulus-anomaly mediation is favored in the unification scenario [35]. In that scenario, the branching fraction of $\mu \rightarrow e \gamma$ becomes larger and the flavor non-universality (as we will describe in Section 10) is needed to satisfy the current bound.

2. type II, $c_R v_R = 1.19 \times 10^{13}$ GeV ($R = 5.1582$) (the best fit)

$$M_{R_1} = 2.4 \times 10^{10} \text{ GeV}, \quad M_{R_2} = 4.6 \times 10^{10} \text{ GeV}, \quad M_{R_3} = 1.1 \times 10^{12} \text{ GeV}, \quad (8.6)$$

$$Y_\nu = \begin{pmatrix} 0.00301 & -0.00147 - 0.00394 i & -0.0031 + 0.0134 i \\ 0.0211 & 0.00023 - 0.0284 i & -0.0073 + 0.0359 i \\ 0.103 & -0.044 - 0.131 i & -0.324 + 0.428 i \end{pmatrix}, \quad (8.7)$$

3. type I, $c_R v_R = 4.69 \times 10^{14}$ GeV ($R = 0.23713$)

$$M_{R_1} = 6.6 \times 10^8 \text{ GeV}, \quad M_{R_2} = 1.3 \times 10^{12} \text{ GeV}, \quad M_{R_3} = 5.5 \times 10^{13} \text{ GeV}, \quad (8.8)$$

$$Y_\nu = \begin{pmatrix} 0.0000957 & 0.000056 - 0.000189 i & 0.00852 - 0.00459 i \\ 0.000222 & 0.0279 - 0.0253 i & 0.0418 - 0.0143 i \\ 0.00400 & -0.0081 + 0.0177 i & -0.02 - 1.11 i \end{pmatrix}, \quad (8.9)$$

4. type I, $c_R v_R = 2.85 \times 10^{13}$ GeV ($R = 2.9853$) (the best fit in type I)

$$M_{R_1} = 6.8 \times 10^9 \text{ GeV}, \quad M_{R_2} = 3.6 \times 10^{11} \text{ GeV}, \quad M_{R_3} = 3.0 \times 10^{12} \text{ GeV}, \quad (8.10)$$

$$Y_\nu = \begin{pmatrix} 0.000443 & 0.00236 + 0.00016 i & 0.0024 + 0.0109 i \\ 0.00302 & -0.00648 - 0.00218 i & 0.0105 + 0.0413 i \\ 0.0208 & 0.100 - 0.0004 i & 0.004 + 0.527 i \end{pmatrix}, \quad (8.11)$$

As explained, the effects from $e^c e^c \Delta_R^{--}$, $e^c \nu^c \Delta_R^-$ couplings are absent in the case 1, and in type I solutions (3 and 4), the contribution from the Majorana coupling is absent. The contribution from the left-handed Majorana coupling has an ambiguity from the Higgs mixings, and here we assume the mixing to make the contributions to the flavor violation maximal. In the figure, the behavior of the plot in case 3 looks different. This is because the (3,3) element of the Dirac neutrino Yukawa coupling is a bit larger than others, and the stop masses are reduced indirectly due to the RGE evolutions, and a larger value of the A -term is needed to reproduce 125 GeV Higgs mass compared to the others. (The (3,3) element in case 1 is also large, but the effect is not large since the 3rd right-handed neutrino is heavy and soon decoupled in the RGE evolution.) The induced off-diagonal elements in the slepton mass matrices are proportional to $3m_0^2 + A_0^2$, and thus, the m_0 dependence of $\text{Br}(\mu \rightarrow e\gamma)$ looks different between the smaller and the larger m_0 . As noted, the value of A_0 is chosen to make the Higgs mass 125 GeV, the detail numerical values depend on the Higgs mass. We note that due to a large value of A_0 (~ 4 -6 TeV), the stau becomes LSP for $m_0 < 600$ GeV. The branching fraction of the case 2 is the largest (in the region satisfying the current experimental bound). This is because the (1,1) and (1,2) elements of the Dirac neutrino Yukawa coupling are larger than the other cases, relating to the result of that the proper size of the down quark mass fit in the case 2.

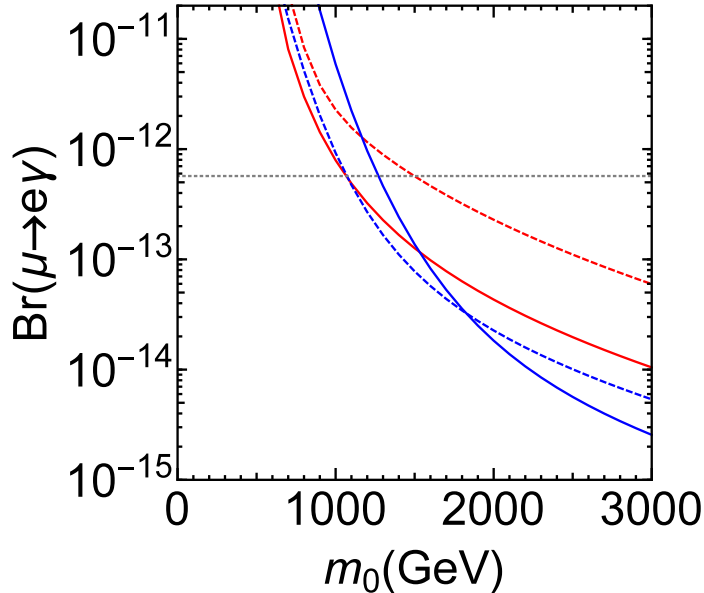


Figure 5: The branching ratio $\mu \rightarrow e\gamma$ for type II at $c_R v_R = 8.86 \times 10^{16}$ GeV ($R = 0.001$) (red solid line), type II at the global minimum ($c_R v_R = 1.19 \times 10^{13}$ GeV) (red dashed line), type I at the local minimum ($c_R v_R = 4.69 \times 10^{14}$ GeV) (blue solid line), and type I at the global minimum ($c_R v_R = 2.85 \times 10^{13}$ GeV) (blue dashed line). We set $\theta_{23} = 0.71$. The gray dashed line shows the current experimental bound, $\text{Br}(\mu \rightarrow e\gamma) < 5.7 \times 10^{-13}$ [36].

Relating to the v_R dependence, we here comment on the electron EDM. We assume A_0 and the Higgsino mass μ to be real because otherwise the EDM becomes much larger than the current experimental bound. Even in the case, if there are e - τ flavor changes (with CP phases) for both left- and right-handed slepton mass matrices, the Bino-Bino diagram can hit the $A_\tau v_d - \mu m_\tau \tan \beta$ for the electron EDM amplitudes, and the value of the EDM can be more than the current experimental bound for slepton masses to be ~ 1 TeV. Surely, if there is only left-handed flavor change such as the case of $c_R v_R = 10^{16}$ GeV, the electron EDM is tiny as long as A_0 and μ are real. Therefore, if the scale of v_R is much less than the unification scale, and the $e^c v^c \Delta_R^-$ coupling can generate the right-handed slepton flavor changing, the electron EDM can be large in the $SO(10)$ model, and the electron EDM can be the probe of the scale v_R .

In the numerical calculation in the above cases, the electron EDM becomes large except for the case 1 for $v_R \sim 10^{16}$ GeV. In the case 2, the current bound of the electron EDM, $|d_e| < 8.7 \times 10^{-29}$ $e \cdot \text{cm}$ [37], can be satisfied for $m_0 > 2.5$ TeV, and then, we obtain $\text{Br}(\mu \rightarrow e\gamma) < 1.1 \times 10^{-13}$. In the case 4 (the best fit in type I), we need $m_0 > 2$ TeV, and then $\text{Br}(\mu \rightarrow e\gamma) < 2.3 \times 10^{-13}$. In the case 1, the electron EDM is tiny ($< 10^{-35}$ $e \cdot \text{cm}$) and

$m_0 \simeq 1$ TeV is still allowed, which can provide the boundary value of the current $\mu \rightarrow e\gamma$ bound.

9 Proton decay

The quark masses and mixings can receive large corrections from the low energy threshold effects. This inversely means that this procedure in the $SO(10)$ model (inputting the lepton parameters and outputting quark masses and mixings) provides a prediction to holomorphic Yukawa couplings for quarks at the unification scale, and the deviations from the observed values of quark masses can be buried by the threshold effects [38, 39, 40]. This feature can be applied to suppress the dimension-five operators in the SUSY GUT models.

The dimension-five operator is given in the form of superpotential as

$$-W_5 = \frac{1}{2}C_L^{ijkl} q_k q_l q_i \ell_j + C_R^{ijkl} e_k^c u_l^c u_i^c d_j^c. \quad (9.1)$$

In the minimal $SU(5)$ GUT model, the Yukawa coupling is given as

$$W_Y = \frac{1}{2}Y_u^{ij} \mathbf{10}_i \cdot \mathbf{10}_j \cdot \mathbf{5}_H + Y_d^{ij} \mathbf{10}_i \cdot \bar{\mathbf{5}}_j \cdot \bar{\mathbf{5}}_H, \quad (9.2)$$

and one obtains

$$C_L^{ijkl} = \frac{1}{M_T} Y_d^{ij} Y_u^{kl}, \quad C_R^{ijkl} = \frac{1}{M_T} Y_d^{ij} Y_u^{kl}, \quad (9.3)$$

where M_T is a triplet Higgs mass. In the $SU(5)$ model, the phases of the eigenvalues of Y_u and Y_d are free (up to an overall phase), and the proton decay four-fermi operator can be canceled among the components of C_L^{ijkl} . In the literature, the right-handed operator, C_R , is often neglected. It is true that the contribution from each component of C_L is larger than C_R because the four-fermi operator from C_R is suppressed due to its Higgsino dressing while the operator from C_L can be generated by the Wino-dressing. However, the contribution to each $p \rightarrow K\bar{\nu}_{e,\mu,\tau}$ from C_L has to be canceled to satisfy the current constraint of the partial proton lifetime, and at that time, the contribution from C_R cannot be neglected since the contribution itself can exceed the current bound, and the minimal $SU(5)$ model is crucially restricted [41, 42]. Due to the reason that the Higgsino dressing hit the Yukawa coupling, the contribution to $p \rightarrow K\bar{\nu}_\tau$ from the right-handed operator is dominated by a single component of $C_R^{1133} \sim y_d y_t / M_T$, in the basis where Y_d is diagonal, and y_d and y_t are down and top quark Yukawa couplings, respectively. Consequently, the partial proton lifetime is bounded, relating to the down quark mass. In the minimal $SU(5)$ model, the down-type quark and the charged-lepton Yukawa coupling matrices are unified ($Y_d = Y_e^T$) at the GUT scale, and thus, one often supposes that the holomorphic coupling is originally Y_e instead of Y_d to generate the dimension-five operator, and a proper down-quark mass is generated by threshold corrections.

In the minimal $SO(10)$ model, the dimension-five operators can be written as [43]

$$C_L^{ijkl} = (M_T^{-1})_{11} \mathbf{h}_{ij} \mathbf{h}_{kl} + (M_T^{-1})_{12} \mathbf{f}_{ij} \mathbf{h}_{kl} + (M_T^{-1})_{31} \mathbf{h}_{ij} \mathbf{f}_{kl} + (M_T^{-1})_{32} \mathbf{f}_{ij} \mathbf{f}_{kl} \quad (9.4)$$

$$= \sum_a \frac{1}{M_a} (X_{a1} \mathbf{h} + X_{a2} \mathbf{f})_{ij} (Y_{a1} \mathbf{h} + Y_{a3} \mathbf{f})_{kl}, \quad (9.5)$$

$$C_R^{ijkl} = (M_T^{-1})_{11} \mathbf{h}_{ij} \mathbf{h}_{kl} - (M_T^{-1})_{12} \mathbf{f}_{ij} \mathbf{h}_{kl} \quad (9.6)$$

$$\begin{aligned} & -((M_T^{-1})_{31} - \sqrt{2}(M_T^{-1})_{41}) \mathbf{h}_{ij} \mathbf{f}_{kl} + ((M_T^{-1})_{32} - \sqrt{2}(M_T^{-1})_{42}) \mathbf{f}_{ij} \mathbf{f}_{kl} \\ & = \sum_a \frac{1}{M_a} (X_{a1} \mathbf{h} - X_{a2} \mathbf{f})_{ij} (Y_{a1} \mathbf{h} - (Y_{a3} - \sqrt{2}Y_{a4}) \mathbf{f})_{kl}, \end{aligned} \quad (9.7)$$

where X and Y are the diagonalization unitary matrices of the colored triplet mass matrix M_T as

$$X M_T Y^T = \text{diag.}(M_1, M_2, \dots, M_5), \quad (9.8)$$

and the mass term of the colored triplets, $(\mathbf{3}, \mathbf{1}, -1/3) + (\bar{\mathbf{3}}, \mathbf{1}, 1/3)$, is

$$- \mathcal{L}_{\text{triplet}} = (H_{\bar{T}}, \bar{\Delta}_{\bar{T}}, \Delta_{\bar{T}}, \Delta'_{\bar{T}}, \Phi_{\bar{T}}) M_T (H_T, \Delta_T, \bar{\Delta}_T, \bar{\Delta}'_T, \Phi_T)^T. \quad (9.9)$$

We note that the right-handed operator can be also generated from other triplets, $(\mathbf{3}, \mathbf{1}, -4/3) + (\bar{\mathbf{3}}, \mathbf{1}, 4/3)$.

The dimension-five operators can be rewritten as linear combinations of $Y_d^{ij} Y_u^{kl}$, $\mathbf{f}_{ij} Y_u^{kl}$, $Y_d^{ij} \mathbf{f}_{kl}$ and $\mathbf{f}_{ij} \mathbf{f}_{kl}$. After fitting the fermion masses and mixings in the minimal $SO(10)$, the phases of the eigenvalues of Y_d and Y_u are no longer free, contrary to the $SU(5)$ model. Instead, the additional contribution, such as $Y_d^{ij} \mathbf{f}_{kl}$, can cancel the proton decay operators choosing the coefficients which is related to the triplet Higgs mixings. However, there are difficulties on the cancellation of the each term as follows:

1. In the fit of fermion masses and mixings, the up quark mass is obtained by a cancellation choosing the doublet Higgs mixing parameter. Therefore, the magnitude of the f_{11} component is thousands of larger than the up quark Yukawa coupling. Then, the $Y_d^{23} f_{11}$ component is too larger for the $p \rightarrow K \bar{\nu}_\tau$ and its coefficient should be small. However, such condition of the Higgs mixing is realized in the (nearly) $SU(5)$ vacua ($r_2 \rightarrow \infty$) of the $SO(10)$ symmetry breaking, which does not realize the fermion masses and mixings. Therefore, if the Higgs contents are restricted, it is hard to suppress the proton decay amplitudes.
2. When the proton decay amplitudes from the C_L operators are cancelled by choosing the coefficients in general $SO(10)$ symmetry breaking vacua, the amplitudes from C_R operator are still very large due to the largeness of f_{11} components. In fact, the signs of the $f_{ij} h_{kl}$ coefficients are opposite between C_L and C_R due to the algebraic reason that the H_T and $\bar{\Delta}_T$ have opposite ‘‘D-parities’’. This fact makes the simultaneous

cancellation of both C_L and C_R unnatural [43]. Depending on the size of f_{11} , the amplitudes of certain decay modes can exceed the current experimental bounds even after canceling the baryon number violating nucleon decay amplitudes by using the full freedom of parameters.

If these issues are seriously taken, the lightest colored Higgs mass should be raised up to suppress the amplitudes by choosing Higgs spectrum [44], and other Higgs multiplet which couples to the fermion multiplets should be employed. For example, if **120** Higgs representation is employed, the up quark Yukawa coupling can be naturally small (relating to the vacua selection) without a cancellation between h and f coupling matrices, and f_{11} element can be made small, which is helpful to reduce the nucleon decay amplitudes [43]. In that mind, we do not perform the cancellation here since it is performed in the literatures [45]. But, we comment that the size of the f_{11} is important for the suppression of the amplitude, and we show the f matrices in our χ^2 minimum fits below.

Here, we show f matrices (in GeV unit) in the form of $rfv_u = F/(1 - r_2)$ to compare with $m_d = Y_d^{11}v_d = rv_u(h + f)_{11}$ in the basis where the down-type quark mass matrix is real (positive) diagonal. We use the χ^2 minimum fits given in the previous sections in the case of $\theta_{23} = 0.71$.

1. type II, $c_R v_R = 8.86 \times 10^{16}$ GeV ($R = 0.001$)

$$rfv_u = \begin{pmatrix} 0.000127 - 0.000015 i & 0.000250 + 0.000026 i & 0.00153 + 0.00565 i \\ 0.000250 + 0.000026 i & 0.00782 - 0.00141 i & 0.0188 - 0.0200 i \\ 0.00153 + 0.00565 i & 0.0188 - 0.0200 i & -0.299 - 0.063 i \end{pmatrix}, \quad (9.10)$$

2. type II, $c_R v_R = 1.19 \times 10^{13}$ GeV ($R = 5.1582$) (the best fit)

$$rfv_u = \begin{pmatrix} 0.00167 - 0.00007 i & -0.000678 + 0.000152 i & -0.00163 - 0.0150 i \\ -0.000678 + 0.000152 i & 0.0312 - 0.00120 i & 0.0437 - 0.0567 i \\ -0.00163 - 0.0150 i & 0.0437 - 0.0567 i & -0.0095 - 0.195 i \end{pmatrix}, \quad (9.11)$$

3. type I, $c_R v_R = 4.69 \times 10^{14}$ GeV ($R = 0.23713$)

$$rfv_u = \begin{pmatrix} 0.0000786 - 0.0000227 i & 0.000228 + 0.000159 i & -0.00206 - 0.00517 i \\ 0.000228 + 0.000159 i & 0.00886 - 0.00080 i & -0.0159 + 0.0204 i \\ -0.00206 - 0.00517 i & -0.0159 + 0.0204 i & -0.357 - 0.049 i \end{pmatrix}, \quad (9.12)$$

4. type I, $c_R v_R = 2.85 \times 10^{13}$ GeV ($R = 2.9853$) (the best fit in type I)

$$rfv_u = \begin{pmatrix} 0.00140 - 0.00025 i & 0.00100 - 0.00019 i & 0.0113 - 0.0208 i \\ 0.00100 - 0.00019 i & 0.0555 + 0.00456 i & 0.00530 + 0.110 i \\ 0.0113 - 0.0208 i & 0.00530 + 0.110 i & 0.065 - 0.505 i \end{pmatrix}. \quad (9.13)$$

As one can see, the 11 elements of the χ^2 minimum fits depend on the scale of $c_R v_R$, and they are large for the $c_R v_R \sim 10^{13}$ GeV. The solutions for the larger v_R scale is more preferable to suppress the nucleon decay amplitudes naturally. In that sense, it is better to apply the larger v_R solutions (instead of the best fits) even though the down quark mass has to be corrected by a threshold effect.

10 Discussion on the modification of Yukawa couplings by threshold corrections

As in the previous sections, in the case $R \sim O(1)$ ($c_R v_R \sim O(10^{13})$ GeV), the down quark mass (and all the other masses and mixings) can be fully fit. In the solution, the (1,1) element of the $\overline{\mathbf{126}}$ Higgs coupling (in the basis where M_d is diagonal) is as large as the down quark Yukawa coupling. On the other hand, the solutions for $R \ll 1$, the (1,1) element can be much less the down quark Yukawa coupling, which has a merit to the natural suppression of the proton decay amplitudes though the fit of the down quark mass deviates from the observation at around 2σ .

In the SUSY models, in addition to the corrections from the RGEs, the finite loop corrections arise due to the SUSY breaking. It is famous that the bottom quark mass can be corrected largely by the finite corrections of the non-holomorphic term. Actually, the quark mass matrices, which are connected to the GUT scale via RGEs, can be modified by the loop correction via the SUSY breaking around TeV scale, and in general, all the quark masses and mixings can be different from them via the RGE evolution. However, the corrections from the loop corrections are severely restricted from the flavor physics data, such as $K-\bar{K}$, $B-\bar{B}$ mixings, $b \rightarrow s\gamma$, and $B_{s,d} \rightarrow \mu^+\mu^-$, and no much room is available. For example, if the bottom quark mass is modified, the $b \rightarrow s\gamma$ and $B_{s,d} \rightarrow \mu^+\mu^-$ processes can be also modified from the SM predictions. If the second generation masses are modified, the $K-\bar{K}$ and/or $D-\bar{D}$ mixings are modified. One may adjust them to the flavor data in general even if there are large corrections in all the quark masses and mixings, but it is not an attractive situation. Among the masses and mixings, only the first generation masses can be modified without a major contradiction to the flavor data, and thus, it is suitable to make the minimal modification to the fit results.

The finite correction of the down-type quark masses from the gluino loop diagram (neglecting the effect from flavor mixings) can be written as

$$\Delta m_{d_i} \simeq \frac{2\alpha_s}{3\pi} m_{\tilde{g}} \sin \theta_{LR}^i \left(F \left(\frac{m_{\tilde{g}}^2}{m_{\tilde{d}_L}^2} \right) - F \left(\frac{m_{\tilde{g}}^2}{m_{\tilde{d}_R}^2} \right) \right), \quad (10.1)$$

where $m_{\tilde{g}}$ is a gluino mass, $F(x) = \log x/(x - 1)$, and θ_{LR} is a left-right mixing angle,

$$\sin \theta_{LR}^i \simeq \frac{A_d^i v_d - \mu m_{d_i} \tan \beta}{m_{d_L^i}^2 - m_{d_R^i}^2}. \quad (10.2)$$

Thus, if the A term is proportional to the Yukawa coupling as in the minimal supergravity model ($A_d^i v_d \simeq A m_{d_i}$), the gluino contribution to the fermion mass is flavor universal :

$$\left(\frac{\Delta m_d}{m_d} \right)_{\text{gluino}} \simeq \left(\frac{\Delta m_s}{m_s} \right)_{\text{gluino}} \simeq \left(\frac{\Delta m_b}{m_b} \right)_{\text{gluino}}. \quad (10.3)$$

The chargino contribution can break the flavor universality to the mass corrections, but the corrections to down and strange quark are still universal. In order to correct the fit of the down quark masses and mixings, we need to break the universality of the corrections, and therefore, the non-proportional term of the trilinear coupling is needed.

In the minimal supergravity model, the scalar potential contains the trilinear coupling originated from the mixed term between the visible and hidden sectors, $W = W_{\text{vis}} + W_{\text{hid}}$, and thus, the scalar trilinear couplings are proportional to the Yukawa couplings. In the string-inspired models, the Yukawa coupling can depend on moduli, τ , and the non-proportional term can be induced,

$$A_{ijk} = A_0(Y_{ijk} + c \partial_\tau Y_{ijk}(\tau)). \quad (10.4)$$

The Yukawa matrix and the derivative of the Yukawa matrix are not necessarily simultaneously diagonalized, and therefore, the non-proportional term can have complete different structure compared to the fermion mass matrix. As a result, the (1,1) element of the non-proportional part of the A term (in the basis of the Yukawa matrix is diagonal) is not necessarily hierarchically small, and it can easily modify the first generation fermion masses. If the gluino and squark masses are around 2 TeV, we estimate that $A_d^{11} \cos \beta$ is sub-GeV to modify the down quark mass. Suppose that the all the components are roughly same order of the trilinear coupling, the corrections to the other elements of the mass matrix are also of the order of 1 MeV, which can be negligible for the generation mixings and the FCNC processes.

If the down quark mass is modified via the trilinear scalar coupling, the up quark mass can be also modified. Therefore, the (1,1) element of the trilinear coupling for the up-type quarks should be small, which is possible within a freedom of the model parameter. Because there are only two Higgs coupling matrices in the minimal model, the (1,1) element of the trilinear coupling for the charged lepton remains in that case, and thus, the electron mass is also modified. The correction to the electron mass is induced by the Bino component of the neutralino, and the modification is not large. Instead, there can have freedom to tune the loop correction of the up quark mass and cancel the tree-level one to make the physical up quark mass tiny. In that case, the cancellation of the proton decay amplitudes described in the previous section can be done at the vacua far from the nearly $SU(5)$ limit.

The scalar trilinear triplet Higgs couplings can induce dimension-four proton decay operators via the triplet Higgs scalar exchange, and the (1,1) element of the coupling can make the excess of the proton decay amplitudes after double gaugino dressing. However, to generate the dimension-four operators, the holomorphic bilinear mass term of the triplet Higgs scalars is needed. Besides, the other elements of the trilinear scalar coupling matrix are free and can be small. Thus, the induced amplitudes can be suppressed within the freedom of the parameters.

As the implication to the low energy observables, the bounds from the neutron EDM need to be considered, as in the case of the minimal flavor violation, and the non-proportional term of the trilinear coupling should be hermitian (in the basis where the quark mass matrix is real/positive diagonal). Because the coupling matrix is symmetric due to the $SO(10)$ algebra, the phases of the components in the non-proportional term are severely restricted. The non-proportional term can be a new source of the flavor violation via the RGE evolution of the scalar masses, and the $\mu \rightarrow e\gamma$ process will be the most stringent constraint on it. As described before, the non-proportional term is not necessarily have a hierarchical structure parallel to the Yukawa hierarchy, and within the freedom, the contributions to $\mu \rightarrow e\gamma$ can be switched off. Rather, choosing the size of (1,2)/(2,1) elements of the trilinear coupling, the size of the $\mu \rightarrow e\gamma$ amplitude can be adjusted, and the production studied in the previous sections becomes just a reference value. However, the qualitative statement relating to the v_R scale dependence is expected to be kept.

We note that the charge/color breaking (CCB) vacua may appear for the large (1,1) element of the scalar trilinear coupling, and the electroweak symmetry breaking vacua may become metastable [46, 47], as similarly to the models in which the fermion masses and mixings are modified by the loop corrections [40]. Surely, if the lifetime of our vacuum can be larger than the age of the universe [48], the model is still valid. The bounds from the tunneling processes of the vacua should be analyzed model-independently, and the bounds are beyond the scope of this paper. We just mention that the vacua may be unstable, but long-lived as in the other analyses.

11 Conclusions and discussions

We study the minimal $SO(10)$ model in which the quarks and leptons couple to only $\mathbf{10}$ and $\overline{\mathbf{126}}$ Higgs representations. One of the main motivation to employ the $\overline{\mathbf{126}}$ Higgs representation is that the Clebsch-Gordan coefficients can naturally explain the Georgi-Jarskog relation, $m_\mu \sim 3m_s$ and $m_e \sim m_d/3$. In fact, the relations are automatic if only (2,2) element is dominated by the $\overline{\mathbf{126}}$ coupling and (1,1), (1,3) elements of the mass matrices are negligible ($\det M_d \sim \det M_e \sim -M_{12}M_{21}M_{33}$). If there is another Yukawa coupling (such as to $\mathbf{120}$ Higgs representation), the relation of the quark and lepton masses can be easily realized. In the minimal Yukawa coupling, on the other hand, the up quark mass is not necessarily small,

and as a consequence, the relation $m_e m_\mu m_\tau \simeq m_d m_s m_b$ is not obvious for a proper size of Cabibbo angle [49]. However, the quark and lepton masses can be fully fit (without such a clear reason) by using the full parameter freedom even in the case of the minimal Yukawa coupling. In fact, as we have described, in the case of $R \sim O(1)$ (i.e. $v_R \sim 10^{13}$ GeV), the freedom is active to fit all of the fermion masses and mixings, which is consistent with the number counting of the parameters.

Even though the fitting of fermion masses and mixings is just a choice of parameters, the minimal $SO(10)$ is still attractive since the model is predictive. As was seen, the scale of v_R is important for the χ^2 minimum fits, and it is related to an intermediate scale determined by the $SO(10)$ symmetry breaking vacua. Although we perform the search of the χ^2 minimum by using the fermion masses at the GUT scale in the minimal SUSY boundary conditions, the qualitative properties of the solutions described in Section 3 are also applied to the case of non-SUSY boundary conditions. In non-SUSY model, the intermediate scale is rather favored for the gauge coupling unification, contrary to the SUSY models, and the constraints from the dimension-five proton decays and the flavor physics are of course absent. To say it inversely, the predicted fermion mass matrices cannot be probed nor applied to the low energy physics in the non-SUSY model. In the sense to probe the GUT scale physics, the SUSY scenario of the predictive minimal Yukawa coupling in the $SO(10)$ model is still attractive and worth to be chased. As it was explained, the solution for $v_R \sim 10^{16}$ GeV is interesting to apply even though the threshold corrections are needed to fit the center value of the down quark mass.

As methodology, physicists often assume the minimality of a model, not only because the model is predictive due to the reduced number of the parameters, but also because the prototypical model can contain the essential features to study the phenomenology of the objects. In general, it is obvious that the predictivity can be obtained by reducing the number of parameters. It is important to dissect the property of the objects to see whether it only originates from the minimality or whether it comes from any other fundamental mechanism theoretically. In reality, the minimality at the GUT scale physics is hard to be verified experimentally, and one can always claim that the corrections can be induced since the reduced Planck scale is just two digit above the GUT scale. Therefore, the concern one has to care about is whether the prediction is stable under the perturbation of the minimality assumption in GUT models, and we should investigate both the speciality of the prediction from the minimality assumption and the essential features which remain predictable even after the model is extended. As described, the major prediction of the minimal $SO(10)$ model (in which the Yukawa coupling to the fermions is minimal) is that the Dirac and Majorana neutrino mass matrices are fully determined. Sometimes, the Higgs contents are also restricted to be minimal, i.e. $\mathbf{10} + \mathbf{126} + \overline{\mathbf{126}} + \mathbf{210}$, and the number of parameters in the Higgs superpotential is made to be minimal in the $SO(10)$ model. In the SUSY version of the minimal Higgs contents, the fermion data fittings require a typical $SO(10)$ symmetry breaking vacuum, and

some decomposed particles from the Higgs multiplets appear at the intermediate scale to obtain the proper size of neutrino masses. The gauge coupling evolution is severely affected by the presence of the particles at the intermediate scales, and the gauge unification suggests a non-SUSY (or split-SUSY) version of the model [15, 18, 19]. In non-SUSY scenario, however, it is impossible to communicate with the predicted fermion mass matrices by using the low energy phenomena, such as the various modes of baryon number violating processes and lepton flavor violation, which are induced by the Yukawa interactions. We, thus, take a stance to probe the footprint of the GUT scale physics by using the SUSY scenario, in which the whole picture of the predicted mass matrices can be influenced to the low energy physics. In order to have the stance, we do not employ the minimality of the Higgs contents. As we have described frequently in this paper, we define the minimal $SO(10)$ model as that based on the minimality of the Yukawa interaction, which is fully predictive to find the structure of the fermion mass matrices.

The important parameters in SUSY GUTs, which can affect low energy physics, are $\mathbf{126}$ vev v_R , $SU(2)_L$ triplet Higgs mass M_Δ , the lightest colored Higgs mass M_{H_C} , and the heavy gauge boson mass M_G . The parameters, v_R , M_Δ , M_{H_C} , and M_G , are functions of the parameters in the Higgs potential and particle spectrum (depending on the consistency of the gauge coupling evolutions) deductively, and one can discuss how the parameters can depend on $SO(10)$ breaking vacua and the particle spectrum [44]. Instead of specifying the Higgs potential and deriving the scale v_R from the certain number of parameters in the Higgs potential, we choose them to be free parameters as methodology because there are plenty of choices to extend the Higgs potential. In fact, v_R is an important scale to describe the GUT symmetry breaking and the neutrino mass spectrum, and it is an open question how the right-handed Majorana neutrino is generated in GUTs and the size of the light neutrino masses are obtained. As we have seen, the fit of the fermion masses and mixings depends on v_R . Actually, the naive scale of the right-handed neutrino masses to reproduce the observation is less than 10^{14} GeV, which is hierarchically smaller than the GUT scale. In other words, the neutrino masses are a bit heavier if the GUT scale, 10^{16} GeV, is considered to be a fundamental scale, and explaining the hierarchy is one of the open questions in GUTs. In the solution of the minimal $SO(10)$ model we feature in this paper, instead of the smallness of the each component of the matrix, the nearly singular Majorana mass matrix is contained for a large scale of v_R . The nearly singular Majorana matrix is one of the solution to explain the neutrino masses keeping the symmetry breaking scale to be 10^{16} GeV, because the inverse of the Majorana mass matrix is included the type I seesaw formulae. In that sense, this solution can provide an approach to the fundamental question, and it is interesting to research the prediction of the model.

In $SU(5)$ GUT, the Dirac neutrino mass matrix is completely independent to the other charged fermions. In the unified model scenario, the hierarchical forms of the Dirac and Majorana neutrino mass matrices are often assumed. The Dirac neutrino mass is generated

by the couplings to the up-type Higgs, and in a certain model, the hierarchy of the Dirac neutrino mass is assumed to be similar to the up-type quarks. The predicted Dirac neutrino Yukawa coupling in the minimal $SO(10)$ model is less hierarchical rather than the up-type quarks, and the hierarchy rather resembles to the down-type quark or charged-leptons. This is simply because the up-type quark mass hierarchy in this model is realized by a cancellation between two Yukawa matrices. Even in the non-minimal models, in which $\mathbf{120}$ Higgs is added to the Yukawa couplings and the (1,1) elements of the Yukawa couplings are assumed to be small to suppress proton decay amplitudes in an $SO(10)$ model, the Dirac neutrino Yukawa coupling also resembles to the down-type quarks and the charged-leptons and the size of the induced FCNCs is similar to the minimal model [32]. In that sense, the size of the induced FCNCs is predictable in the renormalizable $SO(10)$ models. This feature provides an important implication to the process of $\mu \rightarrow e\gamma$ in SUSY models, and it can be tested by the experiment.

As described in the text, the electron EDM is one of the major implications of the v_R dependence in the $SO(10)$ model. If the scale v_R is less than the unification scale, the flavor violation is generated in both left- and right-handed slepton mass matrices, and the electron EDM is enlarged. If the source of the flavor violation is hermitian, the phase of the EDM amplitude is canceled. In the minimal model, the Yukawa coupling is symmetric due to the $SO(10)$ algebra, and the components are not real numbers to reproduce the KM phase. Therefore, the electron EDM can be induced in general for the lower scale v_R . On the other hand, the Yukawa coupling to the $\mathbf{120}$ representation is anti-symmetric, and thus, there can be room to generate the hermitian flavor violation in the non-minimal models. Consequently, the electron EDM can be a major probe to distinguish the models.

Among the quark-lepton phenomena directly induced by the Yukawa interaction, the CP violation in the neutrino oscillations is the last piece to be discovered. In fact, the ongoing experiments have already given the hint that CP is violated in the oscillations, and it is expected that the CP phase (PMNS phase) is measured in the near future. Remarkably, the minimal $SO(10)$ model has predicted the proper size of neutrino 13-mixing angle (before its measurement), which is consistent with the current experimental results. We show the prediction of the PMNS phase in the minimal $SO(10)$ model, in which there are disfavored region depending on the 23-mixing. Now the prediction of the PMNS phase of the model is being challenged to the experimental results, including the precise measurement of the 23-mixing.

A Appendix : Square root matrix

A square root matrix of A , denoted as \sqrt{A} , is defined to be matrices which satisfy $(\sqrt{A})^2 = A$.

In our numerical practical reason, we assume that the eigenvalues of a 3×3 matrix A ,

$\lambda_{1,2,3}$, are not degenerate. Then, it can be diagonalized by a matrix V :

$$A = V \begin{pmatrix} \lambda_1 & & \\ & \lambda_2 & \\ & & \lambda_3 \end{pmatrix} V^{-1}. \quad (\text{A.1})$$

The square root matrix can be expressed as

$$\sqrt{A} = V \begin{pmatrix} \pm\sqrt{\lambda_1} & & \\ & \pm\sqrt{\lambda_2} & \\ & & \pm\sqrt{\lambda_3} \end{pmatrix} V^{-1}. \quad (\text{A.2})$$

The double-signs are in no particular order (INPO), and there are 8-fold matrices for the square root of a 3×3 matrix.

Defining matrices Λ_i as

$$\Lambda_1 = V \begin{pmatrix} 1 & & \\ & 0 & \\ & & 0 \end{pmatrix} V^{-1}, \quad \Lambda_2 = V \begin{pmatrix} 0 & & \\ & 1 & \\ & & 0 \end{pmatrix} V^{-1}, \quad \Lambda_3 = V \begin{pmatrix} 0 & & \\ & 0 & \\ & & 1 \end{pmatrix} V^{-1}, \quad (\text{A.3})$$

we obtain

$$A = \lambda_1 \Lambda_1 + \lambda_2 \Lambda_2 + \lambda_3 \Lambda_3. \quad (\text{A.4})$$

One can easily obtain the following relations:

$$\Lambda_1 + \Lambda_2 + \Lambda_3 = \mathbf{1}, \quad \Lambda_i \Lambda_j = \Lambda_i \delta_{ij}. \quad (\text{A.5})$$

By solving the simultaneous equation

$$\begin{pmatrix} 1 & 1 & 1 \\ \lambda_1 & \lambda_2 & \lambda_3 \\ \lambda_1^2 & \lambda_2^2 & \lambda_3^2 \end{pmatrix} \begin{pmatrix} \Lambda_1 \\ \Lambda_2 \\ \Lambda_3 \end{pmatrix} = \begin{pmatrix} \mathbf{1} \\ A \\ A^2 \end{pmatrix}, \quad (\text{A.6})$$

we obtain¹¹

$$\Lambda_1 = \frac{1}{(\lambda_1 - \lambda_2)(\lambda_1 - \lambda_3)} (A^2 - (\lambda_2 + \lambda_3)A + \lambda_2 \lambda_3 \mathbf{1}), \quad (\text{A.8})$$

$$\Lambda_2 = \frac{1}{(\lambda_2 - \lambda_1)(\lambda_2 - \lambda_3)} (A^2 - (\lambda_1 + \lambda_3)A + \lambda_1 \lambda_3 \mathbf{1}), \quad (\text{A.9})$$

$$\Lambda_3 = \frac{1}{(\lambda_3 - \lambda_1)(\lambda_3 - \lambda_2)} (A^2 - (\lambda_1 + \lambda_2)A + \lambda_1 \lambda_2 \mathbf{1}). \quad (\text{A.10})$$

¹¹ We note that in the case where A is a Hermit matrix, we obtain $(\Lambda_k)_{ij} = V_{ik} V_{jk}^*$ because $V^{-1} = V^\dagger$, and we can express the diagonalization matrix algebraically as

$$V = \begin{pmatrix} \frac{\sqrt{(\Lambda_1)_{11}}}{(\Lambda_1)_{21}} & \frac{\sqrt{(\Lambda_2)_{11}}}{(\Lambda_2)_{21}} & \frac{\sqrt{(\Lambda_3)_{11}}}{(\Lambda_3)_{21}} \\ \frac{\sqrt{(\Lambda_1)_{11}}}{(\Lambda_1)_{31}} & \frac{\sqrt{(\Lambda_2)_{11}}}{(\Lambda_2)_{31}} & \frac{\sqrt{(\Lambda_3)_{11}}}{(\Lambda_3)_{31}} \\ \frac{\sqrt{(\Lambda_1)_{11}}}{\sqrt{(\Lambda_1)_{11}}} & \frac{\sqrt{(\Lambda_2)_{11}}}{\sqrt{(\Lambda_2)_{11}}} & \frac{\sqrt{(\Lambda_3)_{11}}}{\sqrt{(\Lambda_3)_{11}}} \end{pmatrix}. \quad (\text{A.7})$$

Using the matrices Λ_i , the square root matrix can be written as

$$\sqrt{A} = \sum_i s_i \sqrt{\lambda_i} \Lambda_i, \quad (\text{A.11})$$

where s_i stands for the sign of each root of eigenvalue, $s_i = \pm 1$.

Acknowledgments

The work of T.F. is supported in part by the Grant-in-Aid for Science Research from the Ministry of Education, Science and Culture of Japan (No. 26247036). The work of K.I. is supported in part by JSPS Research Fellowships for Young Scientists. The work of Y.M. is supported by the Excellent Research Projects of National Taiwan University under grant number NTU-EPR-104R8915.

References

- [1] G. Aad *et al.* [ATLAS Collaboration], Phys. Lett. B **716**, 1 (2012) [arXiv:1207.7214 [hep-ex]]; S. Chatrchyan *et al.* [CMS Collaboration], Phys. Lett. B **716**, 30 (2012) [arXiv:1207.7235 [hep-ex]]; G. Aad *et al.* [ATLAS and CMS Collaborations], Phys. Rev. Lett. **114**, 191803 (2015) [arXiv:1503.07589 [hep-ex]].
- [2] F. P. An *et al.* [DAYA-BAY Collaboration], Phys. Rev. Lett. **108**, 171803 (2012) [arXiv:1203.1669 [hep-ex]]; J. K. Ahn *et al.* [RENO Collaboration], Phys. Rev. Lett. **108**, 191802 (2012) [arXiv:1204.0626 [hep-ex]]; K. Abe *et al.* [T2K Collaboration], Phys. Rev. Lett. **107**, 041801 (2011) [arXiv:1106.2822 [hep-ex]].
- [3] P. Adamson *et al.* [MINOS Collaboration], Phys. Rev. Lett. **110**, no. 17, 171801 (2013) [arXiv:1301.4581 [hep-ex]]; M. Wilking [T2K Collaboration], PoS EPS - **HEP2013**, 536 (2013) [arXiv:1311.4114 [hep-ex]]; Talk by M. R. Salzgeber at the European Physical Society Conference on High Energy Physics (EPS-HEP2015) in Vienna in July, 2015; D. S. Ayres *et al.* [NOvA Collaboration], hep-ex/0503053; http://theory.fnal.gov/jetp/talks/20150806_nova_docdb.pdf.
- [4] H. Fritzsch and P. Minkowski, Annals Phys. **93**, 193 (1975).
- [5] K. S. Babu and R. N. Mohapatra, Phys. Rev. Lett. **70**, 2845 (1993) [hep-ph/9209215].
- [6] K. Matsuda, Y. Koide and T. Fukuyama, Phys. Rev. D **64**, 053015 (2001) [hep-ph/0010026]; K. Matsuda, Y. Koide, T. Fukuyama and H. Nishiura, Phys. Rev. D **65**, 033008 (2002) [Erratum-ibid. D **65**, 079904 (2002)] [hep-ph/0108202].

- [7] T. Fukuyama and N. Okada, JHEP **0211**, 011 (2002) [hep-ph/0205066].
- [8] T. E. Clark, T. K. Kuo and N. Nakagawa, Phys. Lett. B **115**, 26 (1982); C. S. Aulakh and R. N. Mohapatra, Phys. Rev. D **28**, 217 (1983); C. S. Aulakh, B. Bajc, A. Melfo, G. Senjanović and F. Vissani, Phys. Lett. B **588**, 196 (2004) [arXiv:hep-ph/0306242].
- [9] T. Fukuyama, A. Ilakovac, T. Kikuchi, S. Meljanac and N. Okada, Eur. Phys. J. C **42**, 191 (2005) [hep-ph/0401213]; Phys. Rev. D **72**, 051701 (2005) [hep-ph/0412348]; B. Bajc, A. Melfo, G. Senjanovic and F. Vissani, Phys. Rev. D **70**, 035007 (2004) [hep-ph/0402122]; Phys. Lett. B **634**, 272 (2006) [hep-ph/0511352]; C. S. Aulakh and A. Girdhar, Nucl. Phys. B **711**, 275 (2005) [hep-ph/0405074]; T. Fukuyama, A. Ilakovac, T. Kikuchi, S. Meljanac and N. Okada, J. Math. Phys. **46**, 033505 (2005) [hep-ph/0405300].
- [10] S. Bertolini, M. Frigerio and M. Malinsky, Phys. Rev. D **70**, 095002 (2004) [hep-ph/0406117]; W. -M. Yang and Z. -G. Wang, Nucl. Phys. B **707**, 87 (2005) [hep-ph/0406221]; S. Bertolini and M. Malinsky, Phys. Rev. D **72**, 055021 (2005) [hep-ph/0504241]; A. S. Joshipura and K. M. Patel, Phys. Rev. D **83**, 095002 (2011) [arXiv:1102.5148 [hep-ph]].
- [11] B. Bajc, G. Senjanovic and F. Vissani, Phys. Rev. Lett. **90**, 051802 (2003) [hep-ph/0210207]; Phys. Rev. D **70**, 093002 (2004) [hep-ph/0402140]; H. S. Goh, R. N. Mohapatra and S. -P. Ng, Phys. Lett. B **570**, 215 (2003) [hep-ph/0303055]; Phys. Rev. D **68**, 115008 (2003) [hep-ph/0308197]; B. Dutta, Y. Mimura and R. N. Mohapatra, Phys. Rev. D **69**, 115014 (2004) [hep-ph/0402113]; Phys. Lett. B **603**, 35 (2004) [hep-ph/0406262].
- [12] K. S. Babu and C. Macesanu, Phys. Rev. D **72**, 115003 (2005) [hep-ph/0505200].
- [13] P. Minkowski, Phys. Lett. **B67**, 421 (1977); T. Yanagida in *Workshop on Unified Theories, KEK Report 79-18*, p. 95 (1979); M. Gell-Mann, P. Ramond and R. Slansky, *Supergravity*, p. 315; Amsterdam: North Holland (1979); S. L. Glashow, *1979 Cargese Summer Institute on Quarks and Leptons*, p. 687; New York: Plenum (1980); R. N. Mohapatra and G. Senjanovic, Phys. Rev. Lett. **44**, 912 (1980).
- [14] J. Schechter and J. W. F. Valle, Phys. Rev. D **22**, 2227 (1980); G. Lazarides, Q. Shafi and C. Wetterich, Nucl. Phys. B **181**, 287 (1981); R. N. Mohapatra and G. Senjanovic, Phys. Rev. D **23**, 165 (1981).
- [15] S. Bertolini, T. Schwetz and M. Malinsky, Phys. Rev. D **73**, 115012 (2006) [hep-ph/0605006].

- [16] M. C. Gonzalez-Garcia, M. Maltoni, J. Salvado and T. Schwetz, JHEP **1212**, 123 (2012) [arXiv:1209.3023 [hep-ph]]; D. V. Forero, M. Tortola and J. W. F. Valle, Phys. Rev. D **90**, no. 9, 093006 (2014) [arXiv:1405.7540 [hep-ph]].
- [17] F. Capozzi, G. L. Fogli, E. Lisi, A. Marrone, D. Montanino and A. Palazzo, Phys. Rev. D **89**, 093018 (2014) [arXiv:1312.2878 [hep-ph]].
- [18] B. Bajc, I. Dorsner and M. Nemevsek, JHEP **0811**, 007 (2008) [arXiv:0809.1069 [hep-ph]].
- [19] S. Bertolini, L. Di Luzio and M. Malinsky, Phys. Rev. D **81**, 035015 (2010) [arXiv:0912.1796 [hep-ph]].
- [20] B. Dutta, Y. Mimura and R. N. Mohapatra, Phys. Rev. D **72**, 075009 (2005) [hep-ph/0507319].
- [21] T. P. Cheng and L. F. Li, Phys. Rev. D **22**, 2860 (1980).
- [22] H. S. Goh, R. N. Mohapatra and S. Nasri, Phys. Rev. D **70**, 075022 (2004) [hep-ph/0408139].
- [23] M. Yoshimura and N. Sasao, Phys. Rev. D **89**, 053013 (2014) [arXiv:1310.6472 [hep-ph]].
- [24] K. Bora, J. Phys. **2**, 2013 [arXiv:1206.5909 [hep-ph]].
- [25] K. A. Olive *et al.* [Particle Data Group Collaboration], Chin. Phys. C **38**, 090001 (2014).
- [26] N. Metropolis, A. W. Rosenbluth, M. N. Rosenbluth, A. H. Teller and E. Teller, J. Chem. Phys. **21**, 1087 (1953); W. K. Hastings, Biometrika **57**, 97 (1970).
- [27] R. H. Swendsen and J.-Sh. Wang, Phys. Rev. Lett. **57**, 2607 (1986).
- [28] J. Elevant and T. Schwetz, arXiv:1506.07685 [hep-ph].
- [29] P. Coloma, H. Minakata and S. J. Parke, Phys. Rev. D **90**, 093003 (2014) [arXiv:1406.2551 [hep-ph]].
- [30] H. Fritzsch, Z. z. Xing and S. Zhou, JHEP **1109**, 083 (2011) [arXiv:1108.4534 [hep-ph]].
- [31] N. Haba, T. Horita, K. Kaneta and Y. Mimura, arXiv:1110.2252 [hep-ph].
- [32] B. Dutta, Y. Mimura and R. N. Mohapatra, Phys. Rev. D **87**, no. 7, 075008 (2013) [arXiv:1302.2574 [hep-ph]].
- [33] F. Borzumati and A. Masiero, Phys. Rev. Lett. **57**, 961 (1986); J. Hisano, T. Moroi, K. Tobe, M. Yamaguchi and T. Yanagida, Phys. Lett. B **357**, 579 (1995) [hep-ph/9501407].

- [34] V. Khachatryan *et al.* [CMS and LHCb Collaborations], *Nature* **522**, 68 (2015) [arXiv:1411.4413 [hep-ex]].
- [35] D. Chowdhury and N. Yokozaki, arXiv:1505.05153 [hep-ph].
- [36] J. Adam *et al.* [MEG Collaboration], *Phys. Rev. Lett.* **110**, 201801 (2013) [arXiv:1303.0754 [hep-ex]].
- [37] J. Baron *et al.* [ACME Collaboration], *Science* **343**, 269 (2014) [arXiv:1310.7534 [physics.atom-ph]].
- [38] J. L. Diaz-Cruz, H. Murayama and A. Pierce, *Phys. Rev. D* **65**, 075011 (2002) [hep-ph/0012275].
- [39] T. Enkhbat, arXiv:0909.5597 [hep-ph]; *AIP Conf. Proc.* **1200**, 936 (2010) [arXiv:0911.2299 [hep-ph]].
- [40] M. Iskrzynski and K. Kowalska, *JHEP* **1504**, 120 (2015) [arXiv:1412.8651 [hep-ph]].
- [41] T. Goto and T. Nihei, *Phys. Rev. D* **59**, 115009 (1999) [hep-ph/9808255].
- [42] H. Murayama and A. Pierce, *Phys. Rev. D* **65**, 055009 (2002) [hep-ph/0108104].
- [43] B. Dutta, Y. Mimura and R. N. Mohapatra, *Phys. Rev. Lett.* **94**, 091804 (2005) [hep-ph/0412105].
- [44] B. Dutta, Y. Mimura and R. N. Mohapatra, *Phys. Rev. Lett.* **100**, 181801 (2008) [arXiv:0712.1206 [hep-ph]].
- [45] H. S. Goh, R. N. Mohapatra, S. Nasri and S. P. Ng, *Phys. Lett. B* **587**, 105 (2004) [hep-ph/0311330]; T. Fukuyama, A. Ilakovac, T. Kikuchi, S. Meljanac and N. Okada, *JHEP* **0409**, 052 (2004) [hep-ph/0406068]; M. Severson, arXiv:1506.08468 [hep-ph].
- [46] J. A. Casas and S. Dimopoulos, *Phys. Lett. B* **387**, 107 (1996) [hep-ph/9606237].
- [47] J. h. Park, *Phys. Rev. D* **83**, 055015 (2011) [arXiv:1011.4939 [hep-ph]].
- [48] A. Kusenko, P. Langacker and G. Segre, *Phys. Rev. D* **54**, 5824 (1996) [hep-ph/9602414].
- [49] B. Dutta, Y. Mimura and R. N. Mohapatra, *Phys. Rev. D* **80**, 095021 (2009) [arXiv:0910.1043 [hep-ph]]; *JHEP* **1005**, 034 (2010) [arXiv:0911.2242 [hep-ph]].